Neuropathic Allodynia Involves Spinal Neurexin-1β-dependent Neuroligin-1/Postsynaptic Density-95/NR2B Cascade in Rats

Tzer-Bin Lin, Ph.D., Cheng-Yuan Lai, B.S., Ming-Chun Hsieh, M.Sc., Jian-Lin Jiang, M.D. Student, Jen-Kun Cheng, M.D., Ph.D., Yat-Pang Chau, Ph.D., Ting Ruan, Ph.D., Gin-Den Chen, M.D., Hsien-Yu Peng, Ph.D.

ABSTRACT

Background: Neuroligin-1 (NL1) forms a complex with the presynaptic neurexin-1β (Nrx1b), regulating clustering of *N*-methyl-D-aspartate receptors with postsynaptic density-95 (PSD-95) to underlie learning-/memory-associated plasticity. Pain-related spinal neuroplasticity shares several common features with learning-/memory-associated plasticity. The authors thereby investigated the potential involvement of NL1-related mechanism in spinal nerve ligation (SNL)–associated allodynia.

Methods: In 626 adult male Sprague–Dawley rats, the withdrawal threshold and NL1, PSD-95, phosphorylated NR2B (pNR2B) expressions, interactions, and locations in dorsal horn (L4 to L5) were compared between the sham operation and SNL groups. A recombinant Nrx1b Fc chimera (Nrx1b Fc, 10 μg, 10 μl, i.t., bolus), antisense small-interfering RNA targeting to NL1 (10 μg, 10 μl, i.t., daily for 4 days), or NR2B antagonist (Ro 25-6981; 1 μM, 10 μl, i.t., bolus) were administered to SNL animals to elucidate possible cascades involved.

Results: SNL-induced allodynia failed to affect NL1 or PSD-95 expression. However, pNR2B expression (mean ± SD from 13.1 ± 2.87 to 23.1 ± 2.52, n = 6) and coexpression of NL1–PSD-95, pNR2B–PSD-95, and NL1-total NR2B were enhanced by SNL (from 10.7 ± 2.27 to 22.2 ± 3.94, 11.5 ± 2.15 to 23.8 ± 3.32, and 8.9 ± 1.83 to 14.9 ± 2.27 at day 7, n = 6). Furthermore, neuron-localized pNR2B PSD-95–pNR2B double-labeled and NL1/PSD-95/pNR2B triple-labeled immunofluorescence in the ipsilateral dorsal horn was all prevented by Nrx1b Fc and NL1-targeted small-interfering RNA designed to block and prevent NL1 expression. Without affecting NL1–PSD-95 coupling, Ro 25-6981 decreased the SNL-induced PSD-95–pNR2B coprecipitation (from 18.7 ± 1.80 to 14.7 ± 2.36 at day 7, n = 6).

Conclusion: SNL-induced allodynia, which is mediated by the spinal NL1/PSD-95/pNR2B cascade, can be prevented by blockade of transsynaptic Nrx1b–NL1 interactions. **(ANESTHESIOLOGY 2015; 123:909-26)**

THE development of long-term potentiation (LTP), an enduring increase in the synaptic efficacy that underlies memory consolidation in brain areas,[1] is associated with the altered expression of cell adhesion molecule (CAM) genes in central synapses. At this location, these genes regulate synaptic strength by recruiting scaffolding proteins, neurotransmitter receptors, and synaptic vesicles in response to the binding of counter receptors across the synapse.[2] The knockout of neuroligins (NLs), a family of CAMs enriched in the postsynaptic densities of rodents,[3–6] results in memory deficits. The presence of specifically spliced NL1, a member of the NL family that specifically localizes to excitatory synapses,[7] is a requirement for LTP expression in hippocampal pyramidal cells,[8] which implies a crucial role for NL1 in the

What We Already Know about This Topic

- Pain-related spinal neuroplasticity resembles memory-associated neuroplasticity
- The clustering of *N*-methyl-D-aspartate receptors in the postsynaptic membrane is critical to neuroplastic changes

What This Article Tells Us That Is New

- It was shown that the association of *N*-methyl-D-aspartate NR2B subunits and postsynaptic density-95 scaffolding protein was enhanced in spinal cord dorsal horn neurons after nerve ligation in rats
- The disruption of neurexin-1β–neuroligin-1 interaction reduced allodynia and NR2B–postsynaptic density-95 interactions in nerve-ligated rats

Dr. Lin and Dr. Cheng contributed equally to this article.

Submitted for publication February 2, 2015. Accepted for publication June 24, 2015. From the Department of Physiology, School of Medicine, College of Medicine, Taipei Medical University, Taipei, Taiwan (T.-B.L.); Graduate Institute of Basic Medical Science, College of Medicine, China Medical University, Taichung, Taiwan (T.-B.L.); Department of Biotechnology, Asia University, Taichung, Taiwan (T.-B.L.); Department of Medicine, Mackay Medical College, New Taipei, Taiwan (C.-Y.L., M.-C.H., J.-L.J., J.-K.C., Y.-P.C., H.-Y.P.); Department of Veterinary Medicine, College of Veterinary Medicine, National Chung-Hsing University, Taichung, Taiwan (C.-Y.L.); Department of Physiology, School of Medicine, College of Medicine, National Taiwan University, Taipei, Taiwan (M.-C.H.); Department of Anesthesiology, Mackay Memorial Hospital, New Taipei, Taiwan (J.-K.C.); School of Medicine, Fu-Jen Catholic University, New Taipei, Taiwan (T.R.); and Department of Obstetrics and Gynecology, Chung-Shan Medical University Hospital, Chung-Shan Medical University, Taichung, Taiwan (G.-D.C.).

 Anesthesiology 2015; 123:909-26

neural plasticity that underlies memory formation. Spinal plasticity caused by damage to the peripheral tissue/nerves shares several common machineries with LTP that result in postinjury pain and hypersensitivity.[9] Although NL1 has been implicated as a key molecule that regulates the forms of LTP in brain areas, the roles of NL1 in spinal plasticity, which allows for enhanced nociception after injury, have not been identified. Therefore, the first aim of this study is to elucidate the contribution of NL1 to the spinal plasticity underlying neuropathic nociceptive hypersensitivity.

Although the mechanism has not been fully elucidated, NL1 may affect LTP by modifying the glutamatergic *N*-methyl-D-aspartate receptor (NMDAR)–mediated synaptic response because NL1 possesses postsynaptic density-95 (PSD-95)/discs large/zona occludens-1–binding motifs in the cytoplasmic domain that interacts with PSD-95[10] to recruit and cluster NMDARs.[11] Moreover, NL knockout mice exhibit diminished NMDAR-mediated synaptic responses[12] and deficits in hippocampal LTP.[13] Our laboratory has demonstrated painful visceral irritation,[14,15] neuropathic injury,[16,17] and enhanced PSD-95 coupling with NR2B-containing NMDARs and subsequent NR2B phosphorylation in the dorsal horn. Conversely, uncoupling PSD-95 from NR2B-containing NMDARs prevents spinal NR2B phosphorylation and ameliorates neuropathic allodynia.[17] These observations prompted us to test whether spinal PSD-95–NR2B coupling–dependent NR2B activation acts downstream of NL1 to mediate the nociceptive hypersensitivity caused by neuropathic injury.

Neurexin-1 (Nrx1), a presynaptic CAM that has longer Nrx1α and shorter Nrx1β (Nrx1b) isoforms,[18,19] was demonstrated to regulate the membrane trafficking of NMDARs,[20] which is crucial for synaptic strength.[21] Transsynaptic Nrx1b–NL1 interactions enhanced the PSD-95-dependent recruitment of postsynaptic molecules in hippocampal[22,23] and cortical neurons.[24] In cultured cells, the expression of Nrx1b enhances the clustering of NMDARs with PSD-95 on the postsynaptic dendrite *via* Nrx1b–NL binding.[23,25,26] Because several studies have demonstrated that the Nrx1b–NL1 interaction modulates the downstream NL1/PSD-95/NMDAR cascade, we hypothesized that Nrx1b contributes to neuropathic injury–induced nociceptive hypersensitivity by interacting with NL1, which subsequently activates the spinal NL1/PSD-95/pNR2B cascade. Accordingly, we tested this hypothesis in an *in vivo* rat model.

Materials and Methods

Animal Preparations

All animal procedures in this study were conducted in accordance with the guidelines of the International Association for the Study of Pain[27] and were reviewed and approved by the institutional review board of Taipei Medical University, Taipei, Taiwan. A total of 626 adult male Sprague–Dawley rats (200 to 250 g) were used throughout this study. Animals were randomly allocated to treatment groups by a computer with the use of a research randomizer, and the sample size of each group was based on our previous experience. In each group, there were 10 rats used for behavioral test, and 6 rats for the Western blot, immunohistochemistry, and coprecipitation analyses; the investigators were blinded to the treatment groups for all experiments. Eight animals showed neurological deficits after the implantation of a catheter; these animals were excluded from the statistical analysis. Therefore, a total of 618 animals were used for the statistical analyses.

Spinal Nerve Ligation

After anesthesia (isoflurane, induction 5% in air, maintenance 2% in air), the left L5 to L6 spinal nerves were dissected and tightly ligated with 6-0 silk sutures 2 to 5 mm distal to the dorsal root ganglia.[17,28] In the sham operation group, the surgical procedures were identical to the nerve ligation group, except the silk sutures were left unligated.

Intrathecal Catheter

Polyethylene-10 silastic tubing was implanted in the lumbar enlargement of the spinal cord. After implantation, the animals were allowed to recover for 3 days, and those that showed neurological deficits after surgery were sacrificed and excluded from the statistical analyses.[17,28]

Behavioral Studies

Tactile sensitivity was assessed by measuring the paw withdrawal threshold of rats in response to probing with von Frey monofilaments.[29] In brief, rats were placed individually in an opaque plastic cylinder, which was placed on a wire mesh. Animals were habituated for 1 h to allow acclimatization to the test environment before each test. After acclimatization, calibrated von Frey filaments (0.07 to 26.0 g) were applied to the plantar surfaces of the hind paws of rats; the animals' tactile thresholds before operation were set to 15 g.[17] The motor function was assessed using an accelerating rota-rod apparatus (LE8500; Ugo Basile, Italy) in some animals. For acclimatization, the animals were subjected to three training trials at 3- to 4-h intervals on 2 separate days. During the training sessions, the rod was set to accelerate from 3 to 30 rpm over a 180-s period. During the test session, the performance times of rats were recorded up to a cutoff time of 180 s. Three measurements obtained at intervals of 5 min were averaged for each test.[30]

Western Blotting

The dissected dorsal horn (L4 to L5) sample was homogenized in 25 mM Tris-HCl, 150 mM NaCl, 1% NP-40, 1% sodium deoxycholate, and 0.1% sodium dodecyl sulfate with a complete protease inhibitor mixture (Roche, Germany). After incubation on ice (1 h), the lysates were centrifuged (14,000 rpm, 20 min, 4°C). The protein concentrations were determined using a bicinchoninic acid assay. In brief, the supernatant was separated on an acrylamide gel

and transferred to a polyvinylidene difluoride membrane, which was then incubated (1 h, room temperature) in either sheep anti-NL1 (1:1,000; R&D, USA), mouse anti-PSD-95 (1:1,000; Millipore, USA), sheep anti-neurexin-1β (1:1,000; R&D), rabbit anti-phosphorylated NR2B (pNR2B 1:1,000; Millipore), or mouse anti-glyceraldehyde 3-phosphate dehydrogenase (1:4,000; Santa Cruz Biotechnology, USA). The blots were washed and incubated (1 h at room temperature) in peroxidase-conjugated goat anti-rabbit immunoglobulin G (IgG) (1:8,000; Jackson ImmunoResearch, USA), goat anti-mouse IgG (1:8,000; Jackson ImmunoResearch), or rabbit anti-sheep IgG (1:8,000; Santa Cruz Biotechnology). The protein bands were visualized using an enhanced chemiluminescence detection kit (ECL Plus; Millipore) and then subjected to a densitometric analysis with Science Lab 2003 (Fuji, Japan).

Coprecipitation

Rabbit polyclonal antibody against PSD-95 or total NR2B was incubated (overnight, 4°C) with the dorsal horn extracts. The 1:1 slurry protein agarose suspension (Millipore) was added into this protein immunocomplex, and the mixture was incubated (2 to 3 h, 4°C). The agarose beads were washed once with 1% (v/v) Triton X-100 in an immunoprecipitation buffer (50 mM Tris-Cl, pH 7.4, 5 mM EDTA, 0.02% [w/v] sodium azide), twice with 1% (v/v) Triton X-100 in an immunoprecipitation buffer containing 300 mM NaCl, and thrice with an immunoprecipitation buffer only. The bound proteins were eluted with sodium dodecyl sulfate polyacrylamide gel electrophoresis sample buffer at 95°C. The proteins were separated by sodium dodecyl sulfate polyacrylamide gel electrophoresis, electrophoretically transferred to polyvinylidene difluoride membranes, and detected using sheep anti-NL1 (1:1,000; R&D), mouse anti-PSD-95 (1:1,000; Millipore), rabbit anti-total NR2B (tNR2B 1:1,000; Millipore), and rabbit anti-pNR2B (1:1,000; Millipore).

Immunofluorescence

Six rats were chosen randomly from each group, and the spinal cord sample of each animal was taken for immunofluorescence. After perfusion (100 ml phosphate-buffered saline followed by 300 ml paraformaldehyde; 4%; pH 7.4), the spinal cord samples were harvested, postfixed (4°C for 4 h), and cryoprotected in sucrose solution (30%) overnight. Starting sections of spinal slices were chosen randomly and every fifth section throughout L4 to L5 was analyzed. The samples were double-labeled to investigate the interactions between NL1 and neuronal/glial/microglia markers; specifically, the spinal sections were incubated overnight (4°C) with a mixture of sheep anti-NL1 (1:200; R&D) and mouse monoclonal antineuronal nuclear antigen (NeuN, a neuronal marker, 1:500; Millipore), mouse antiglial fibrillary acidic protein (GFAP, a marker of astroglial cells; 1:1,000; Millipore), or mouse anti-integrin αM (OX-42, a marker of microglia; 1:500; Santa Cruz Biotechnology). For the double-labeling analyses that examined the interactions between PSD-95 and pNR2B, the spinal sections were incubated overnight (4°C) with a mixture of mouse anti-PSD-95 (1:200; Santa Cruz Biotechnology) and rabbit anti-pNR2B (1:200; Millipore). For the triple-labeling analyses that examined the interactions between NL1, PSD-95, and pNR2B, the spinal sections were incubated overnight (4°C) with a mixture of sheep anti-NL1 (1:100; R&D), mouse anti-PSD-95 (1:200; Santa Cruz Biotechnology), and rabbit anti-pNR2B (1:200; Millipore). The sections were then incubated (1 h, 37°C) with Alexa Fluor 405 (blue, 1:1,500; Life Technologies, USA), Alexa Fluor 488 (green, 1:1,500; Life Technologies), and Alexa Fluor 594 (red, 1:1,500; Life Technologies). The sections were subsequently rinsed in phosphate-buffered saline, and coverslips were applied. When these fluorescent markers are excited, they can be easily detected by a camera-coupled device (X-plorer; Diagnostic Instruments, Inc., USA) through a fluorescent microscopy (LEICA DM2500, Germany). Five sections from the neuropathic or sham-operated spinal cord were used for cell counting in each rat. Cell counting was carried out under a microscope at the magnification of ×200.

Small-interfering RNA

The 19 nucleotide duplexes of the small-interfering RNAs (siRNAs) for NL1 were 5′-GUUGAUAAUUUAUAUGGAU-3′ and the missense nucleotides were 5′-AUCCAUAUAAAUUAUCAAC-3′. The missense or siRNA was intrathecally administered with a polyethyleneimine (10 μl, 25 kDa; Sigma–Aldrich, Germany)-based gene delivery system into the dorsal subarachnoid space (L4 to L5) of animals through the implanted catheter (daily for 4 days from day 3 to 6 after spinal nerve ligation [SNL]).

Drugs Application

Ro 25-6981 (a NR2B activation antagonist; 100 nM, 10 μl; Tocris Bioscience, USA; bolus at 7 days after SNL; intrathecal) and Nrx1b Fc (Neurexin-1β Fc chimera; Recombinant Human Neurexin 1β Fc Chimera; which does not include the splice site 4 insertion and shares 99% amino acid sequence identity with rat NRX1b; I, 3 and 5 μg; 10 μl; R&D; bolus at 7 days after SNL; intrathecal) were administered intrathecally *via* a bolus injection. A vehicle solution of a volume identical to that of the tested agents was dispensed to serve as a control.

Data Analysis

All data in this study were analyzed using SigmaPlot 10.0 (Systat Software, USA) or Prism 6.0 (GraphPad, USA) and are expressed as the mean ± SD. A paired two-tailed Student *t* test was used to compare the means between groups. The paw withdrawal threshold, protein abundance, and mRNA abundance measured at an identical time point was analyzed using one-way ANOVA. The effects of operations and/or treatments were assayed using two-way ANOVA of groups by comparing value repeated measured at time points after

operations/treatments, and *post hoc* Tukey tests were used to compare the means of groups. Significance was set at a *P* value less than 0.05.

Results

Nerve Ligation–induced Behavioral Allodynia

We initially examined whether SNL induces behavioral allodynia using von Frey tests. Although SNL failed to affect the response of the contralateral hind paw (fig. 1A; SNL CONTRA; 15.7 ± 5.89, 14.6 ± 4.65, 14.6 ± 4.65, 15.7 ± 5.89, and 15.1 ± 4.36 at days 1, 3, 7, 14, and 21, respectively, compared with day −1), it provoked allodynia, as evidenced by significant decreases in the withdrawal threshold of the ipsilateral hind paw (SNL IPSI; 5.4 ± 2.12, 0.9 ± 0.53, 0.3 ± 0.39, 0.3 ± 0.27, and 0.3 ± 0.38 at days 1, 3, 7, 14, and 21, respectively, n = 10) when compared with the presurgery measurement (day −1). Time-dependent analyses demonstrated that the decrement in the withdrawal threshold began at day 1, peaked at day 7, and remained relatively constant for at least 21 days postsurgery. Nevertheless, the sham operation failed to affect the withdrawal thresholds of the ipsilateral or contralateral hind paws at these time points (sham IPSI and sham CONTRA, respectively; sham IPSI, 15.7 ± 5.89, 15.2 ± 6.16, 15.7 ± 5.89, 16.2 ± 5.55, and 15.2 ± 6.16 and sham CONTRA, 15.1 ± 4.36, 15.6 ± 4.62, 15.2 ± 6.16, 14.6 ± 4.65, and 14.6 ± 4.65 at days 1, 3, 7, 14, and 21, respectively, compared with day −1, both n = 10). These results suggest that our experimental nerve injury model selectively induced allodynia in the ipsilateral hind paw.

Nerve Ligation Did Not Affect Spinal NL1 Expression

Following our observation of SNL-provoked allodynia, we measured the abundance of spinal NL1 in response to the experimental neuropathic injury. Unexpectedly, the Western blotting analyses demonstrated that neither SNL nor the sham operation affected NL1 expression in the ipsilateral dorsal horn (L4 to L5) on days 3, 7, 14, or 21 compared with the presurgery controls (fig. 1, B and C; day −1, sham IPSI, 9.7 ± 2.62, 10.0 ± 2.03, 9.1 ± 2.40, and 10.3 ± 2.38, respectively, compared with day −1, n = 6; SNL IPSI, 8.8 ± 2.65, 9.3 ± 2.88, 9.4 ± 2.27, and 9.6 ± 2.64, respectively, compared with day −1, n = 6). Moreover, the reverse transcription–polymerase chain reaction results demonstrated no changes in the mRNA levels at these time points in either group compared with the presurgery measurements (fig. 1D; sham IPSI, 1.0 ± 0.33, 1.1 ± 0.32, 1.0 ± 0.44, and 1.0 ± 0.32 at days 3, 7, 14, and 21, respectively, compared with day −1, n = 6; SNL IPSI, 1.2 ± 0.33, 1.3 ± 0.31, 1.1 ± 0.35, and 1.2 ± 0.43 at days 3, 7, 14, and 21, respectively, compared with day −1, n = 6). These results indicate that the SNL-induced allodynia did not correlate with spinal NL1 expression.

SNL-induced Interactions between Spinal NL1 and PSD-95

The interaction between NL1 and PSD-95 regulates intracellular signals that mediate neural activity[10,31]; moreover, our previous study demonstrated that spinal PSD-95 plays an important role in the development of neuropathic allodynia.[32] Therefore, we hypothesized that the spinal NL1–PSD-95 interaction contributes to the nociceptive hypersensitivity caused by neuropathic injury. To test this hypothesis, we compared the relative amounts of PSD-95-bound NL1 at different time points before and after surgery. In the PSD-95 immunoprecipitates (IP:PSD-95; purified from the ipsilateral dorsal horn samples; fig. 1, E and F), SNL, but not the sham operation, significantly increased the amount of PSD-95-bound NL1 (PSD-95–NL1) in the ipsilateral dorsal horn at day 3, 7, 14, and 21 after SNL (sham IPSI, 13.1 ± 4.86, 11.2 ± 2.97, 11.7 ± 2.85, and 12.2 ± 4.19; SNL IPSI, 19.2 ± 4.44, 25.2 ± 5.51, 22.0 ± 5.25, and 19.2 ± 4.64 at days 3, 7, 14, and 21, respectively, compared with day −1, both n = 6). The SNL-increased PSD-95–NL1 interaction was parallel to the time course of decrements in withdrawal latency. In contrast, PSD-95 immunoreactivity (PSD-95-PSD-95) was stable at all time points in both groups (sham IPSI, 10.8 ± 2.88, 12.0 ± 2.20, 10.8 ± 2.18, and 10.6 ± 2.63 and SNL IPSI, 11.2 ± 2.68, 11.6 ± 2.55, 11.7 ± 2.47, and 12.0 ± 2.41 at days 3, 7, 14, and 21, respectively, compared with day −1, both n = 6). In consistence, the immunohistochemistry analyses of the ipsilateral dorsal horns (L4 to L5; dissected on day 7 postsurgery) did not reveal a significant difference in the numbers of NL1-positive neurons between the SNL (fig. 2, A and B; SNL 7D, 30.5 ± 9.35, n = 6) and sham-operated groups (sham 7D, 33.3 ± 13.49, n = 6). Moreover, the double-staining results demonstrated that the immunofluorescence of NL1 colocalized with that of PSD-95 in the dorsal horn of SNL rats. When spinal slices were labeled for NL1 and NeuN (a neuron marker), OX-42 (a microglia marker), or GFAP (an astrocyte marker), the double-staining images revealed that the NL1 immunofluorescence overlapped with that of NeuN but not OX-42 or GFAP, which implies that the NL1 immunofluorescence occurred in dorsal horn neurons and not in the glia or astrocytes. Together, these results indicated that SNL enhanced spinal NL1–PSD-95 coupling in dorsal horn neurons but did not affect NL1.

SNL Provoked NR2B Phosphorylation Colocalized with PSD-95

Previous studies have demonstrated that interactions between NL1 and PSD-95 recruit and cluster NMDARs[11] that enable the subsequent phosphorylation of specific NMDAR subunits.[33] Our laboratory has shown that SNL-induced dorsal horn PSD-95–NR2B coupling and subsequent NR2B phosphorylation play a role in the development of neuropathic pain.[17] Because our data indicate that the physical coupling between NL1 and PSD-95 contributes to neuropathic allodynia, we tested whether SNL provoked spinal NL1–PSD-95–pNR2B interactions by first examining the cellular distributions of spinal PSD-95 and pNR2B in response to SNL. Although SNL did not

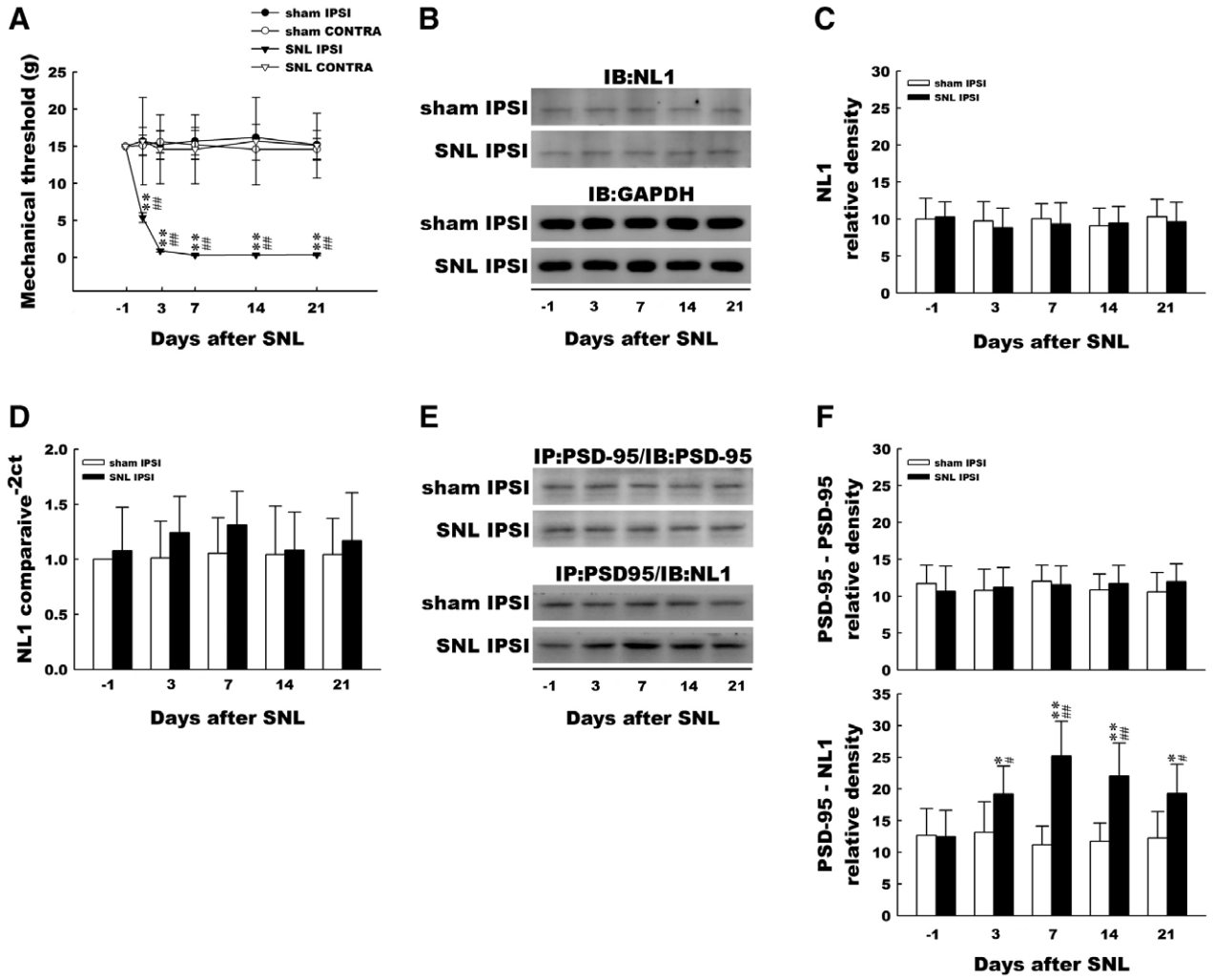

Fig. 1. Nerve ligation induces behavioral allodynia and spinal neuroligin-1 (NL1)–postsynaptic density-95 (PSD-95) coupling. (*A*) Spinal nerve ligation (SNL; SNL IPSI) but not the sham operation (sham IPSI) significantly decreased the mechanical threshold of the ipsilateral hind paw at days 1, 3, 7, 14, and 21 postsurgery. Neither the sham operation (sham CONTRA) nor the SNL (SNL CONTRA) affected the mechanical threshold of the contralateral hind paw across the postsurgery timeline (***P* < 0.01 *vs.* sham IPSI, ##*P* < 0.01 *vs.* day −1, n = 10). (*B*) The time course of NL1 expression in the ipsilateral dorsal horn after SNL. The level of glyceraldehyde 3-phosphate dehydrogenase (GAPDH) protein was used as a loading control. (*C*) Neither the SNL nor the sham affected NL1 expression in the ipsilateral dorsal horn postsurgery. (*D*) In both the SNL and sham groups, no significant differences were evident in NL1 mRNA expression in the ipsilateral dorsal horn postsurgery as calculated with the $2^{-\Delta\Delta Ct}$ ($^{-2ct}$) method. (*E*) The time course of PSD-95–NL1 coupling after SNL. (*F*) In contrast to the stable PSD-95 immunoreactivity postsurgery in both groups, SNL enhanced PSD-95-bound NL1 in the ipsilateral dorsal horn samples on days 3, 7, 14, and 21 postsurgery (**P* < 0.05, ***P* < 0.01 *vs.* sham IPSI, #*P* < 0.05, ##*P* < 0.01 *vs.* day −1, n = 6). CONTRA = contralateral; IB = immunoblot; IP = immunoprecipitate; IPSI = ipsilateral.

affect PSD-95 immunofluorescence (fig. 3, A and B), it significantly enhanced the pNR2B immunofluorescence that colocalized with PSD-95 at 7 days after surgery compared with the sham operation (PSD-95, 32.0 ± 8.69 in SNL 7D compared with 28.7 ± 10.9 in sham 7D, n = 6; pNR2B, 75.3 ± 14.36 in SNL 7D compared with 22.0 ± 9.42 in sham 7D, n = 6; PSD-95/pNR2B, 19.8 ± 7.25 in SNL 7D compared with 8.17 ± 3.97 in sham 7D, n = 6), which indicated that SNL-enhanced NR2B phosphorylation coincided with PSD-95 in the dorsal horn neurons. Our previous study has shown that SNL time-dependently provoked allodynia and pNR2B expression with a maximal effect at 7 days after surgery.[17] We next confirmed the effects of SNL on the expressions of candidate proteins, and the results of Western blotting experiments demonstrated that SNL provoked dorsal horn NR2B phosphorylation as evidenced by a significant increase in the band intensity of pNR2B (fig. 3, C and D; pNR2B; 23.1 ± 2.52 in SNL 7D compared with 13.1 ± 2.87 in sham 7D, n = 6). However, SNL did not affect the NL1 or PSD-95 level (NL1, 13.5 ± 3.30 in SNL 7D compared with 13.8 ± 3.33 in sham 7D, n = 6; PSD-95, 20.4 ± 2.9 in SNL 7D compared with

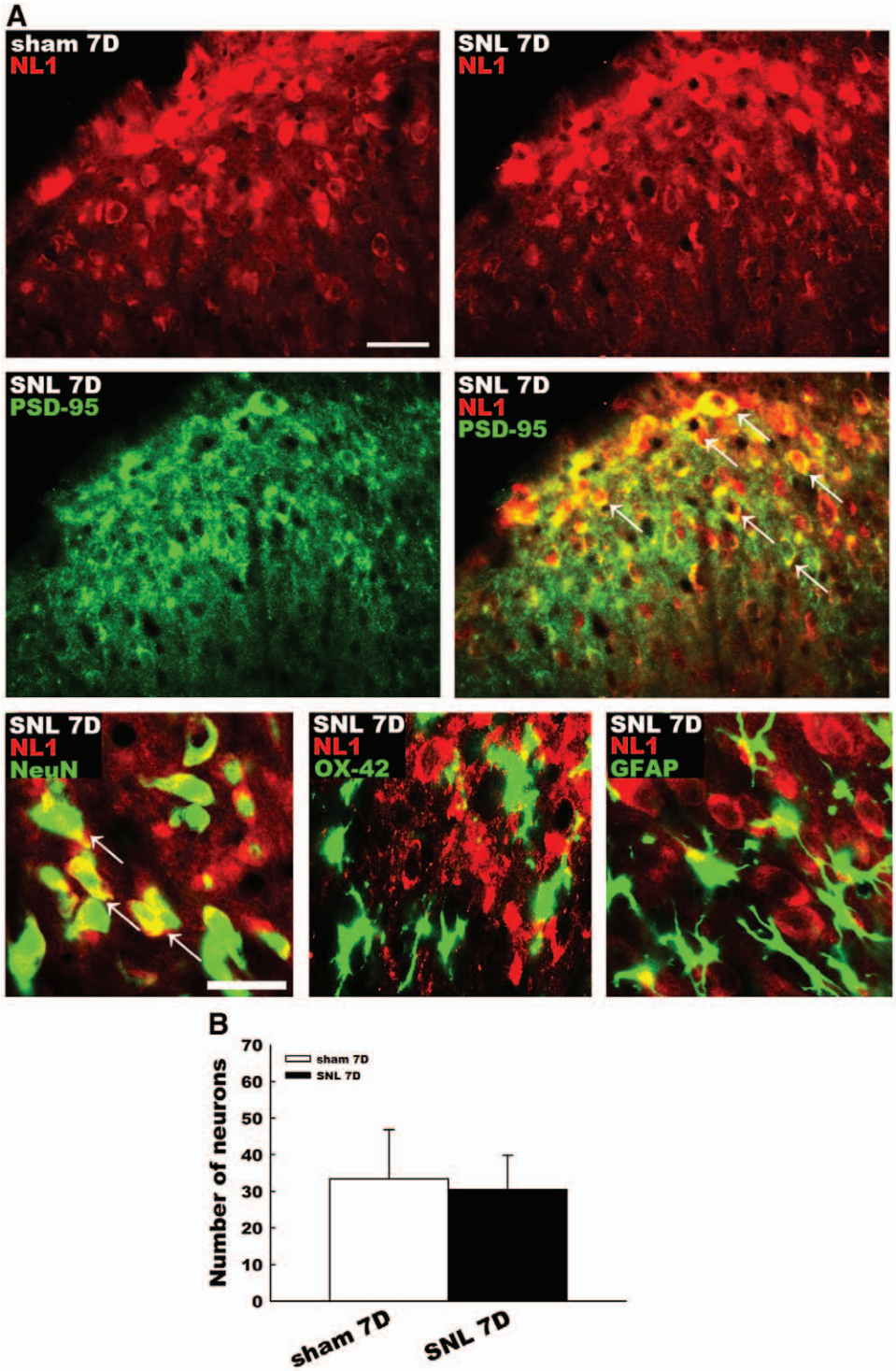

Fig. 2. Colocalized neuroligin-1 (NL1) and postsynaptic density-95 (PSD-95) immunoreactivity in dorsal horn neurons. (*A*) The NL1 immunoreactivity (*red*) in the ipsilateral dorsal horn of the spinal cord sections obtained on day 7 postsurgery exhibited no differences between the spinal nerve ligation (SNL 7D) and sham-operated (sham 7D) animals. The PSD-95 (*green*) fluorescence was coincident with NL1 (*yellow*; indicated by *arrows*); and NL1 immunoreactivity (*red*) colocalized (*yellow*) with NeuN (*green*, a marker of neurons; indicated by *arrows*) but not OX-42 (*green*, a marker of microglia) or glial fibrillary acidic protein (GFAP; *green*, a marker of astrocytes). Each of these images is representative of six sample preparations, and similar results were observed each time. *Scale bar* = 50 μm, thickness = 50 μm. (*B*) The numbers of NL1-positive neurons in the ipsilateral dorsal horn measured 7D postsurgery did not vary between the SNL and sham-operated groups.

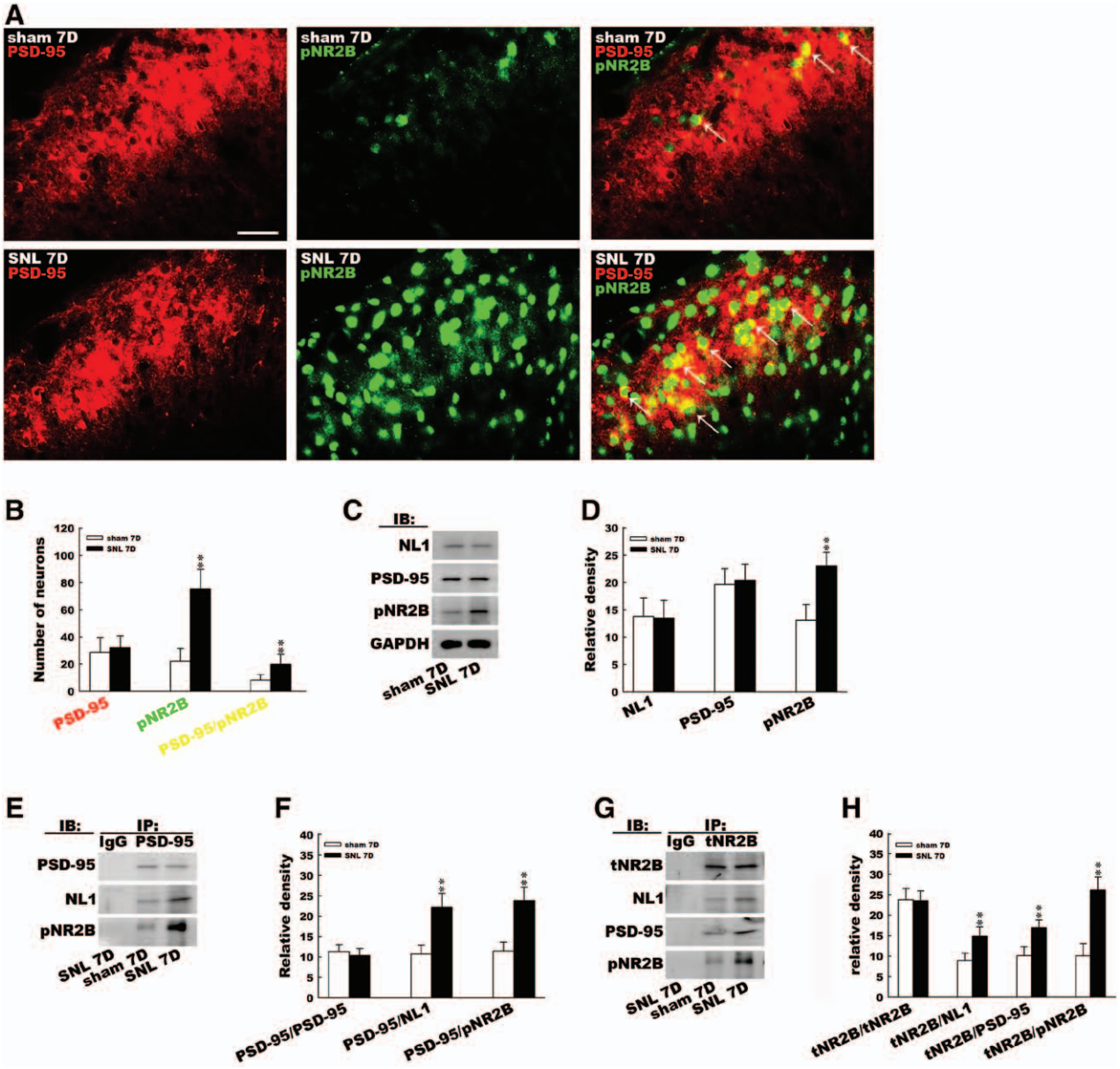

Fig. 3. Nerve ligation induces the interactions between neuroligin-1 (NL1), postsynaptic density-95 (PSD-95), and phosphorylated NR2B (pNR2B). (*A*) At day 7 (7D) postsurgery, although it elicited no effect on that of PSD-95 (*red*), spinal nerve ligation (SNL; SNL 7D) but not the sham operation (sham 7D) notably enhanced the immunofluorescence of pNR2B (*green*) in the ipsilateral dorsal horns. The immunofluorescence of pNR2B colabeled with that of PSD-95 in both the SNL and sham-operated groups (*yellow*, indicated by *arrows*); and there were more colabeled neurons in the SNL than the sham-operated group. Each of these images is representative of six sample preparations. *Scale bar* = 50 μm, thickness = 50 μm. (*B*) SNL enhanced numbers of pNR2B-positive and PSD-95/pNR2B double-labeled neurons (***P* < 0.01 *vs.* sham 7D, n = 6). (*C*) Immunoblot (IB) for NL1, PSD-95, and pNR2B after SNL. The level of glyceraldehyde 3-phosphate dehydrogenase (GAPDH) was used as a loading control. (*D*) Although it elicited no effect on the expressions of NL1 or PSD-95, SNL up-regulated the level of pNR2B in the ipsilateral dorsal horn (***P* < 0.01 *vs.* sham 7D, n = 6). (*E*) Coprecipitation of PSD-95 with NL1 and pNR2B in the ipsilateral spinal cord after SNL. No immunoreactivity for the candidate proteins was detected in the immunoglobulin G (IgG)-recognized precipitates. (*F*) Although it elicited no effect on PSD-95 immunoreactivity, SNL significantly increased the amounts of PSD-95-bound NL1 and pNR2B (***P* < 0.01 *vs.* sham 7D, n = 6). (*G*) Coprecipitation of total NR2B (tNR2B) with NL1, PSD-95, and pNR2B in the ipsilateral spinal cord after SNL. No immunoreactivity for the candidate proteins was detected in the IgG-recognized precipitates. (*H*) Although it elicited no effect on tNR2B immunoreactivity, SNL significantly increased the amounts of tNR2B-bound NL1, PSD-95, and pNR2B (***P* < 0.01 *vs.* sham 7D, n = 6). IP = immunoprecipitate.

19.6 ± 2.86 in sham 7D, n = 6). These findings indicated that SNL induced spinal NR2B phosphorylation without affecting NL1 or PSD-95 expression.

SNL Provoked Interactions between Spinal NL1, PSD-95, and pNR2B

In the PSD-95 immunoprecipitates (IP:PSD-95; fig. 3, E and F) that were purified from the ipsilateral dorsal horn samples (L4 to L5; day 7 postsurgery), the PSD-95 immunoreactivity was found to be similar between the sham-operated and SNL animals (PSD-95/PSD-95, 10.4 ± 1.69 in SNL 7D compared with 11.3 ± 1.69 in sham 7D, n = 6). In contrast, SNL increased the amounts of PSD-95-bound NL1 and pNR2B, as evidenced by the significant increase in the immunoreactivities in the precipitates compared with the sham operation (PSD-95/NL1, 22.2 ± 3.39 in SNL 7D compared with 10.7 ± 2.27 in sham 7D, n = 6; PSD-95/pNR2B, 23.8 ± 3.32 in SNL 7D compared with 11.4 ± 2.15 in sham 7D, n = 6). Similarly, although the tNR2B immunoreactivity did not differ between groups (fig. 3, G and H; tNR2B/tNR2B, 23.5 ± 2.43 in SNL 7D compared with 23.8 ± 2.75 in sham 7D, n = 6), SNL significantly increased the amounts of tNR2B-bound NL1, PSD-95, and pNR2B in the tNR2B precipitates (IP:tNR2B) compared with the sham-operated controls (tNR2B/NL1, 14.9 ± 2.27 in SNL 7D compared with 8.9 ± 1.83 in sham 7D, n = 6; tNR2B/PSD-95, 16.9 ± 1.90 in SNL 7D compared with 10.1 ± 2.17 in sham 7D, n = 6; tNR2B/pNR2B, 26.1 ± 3.20 in SNL 7D compared with 10.1 ± 3.02 in sham 7D, n = 6). In the nonspecific IgG-recognized immunoprecipitates (IP:IgG), immunoreactivities to antibodies against NL1, PSD-95, or pNR2B were not detectable. These results indicated that SNL induced physical interactions between NL1, PSD-95, and pNR2B in the dorsal horn.

NL1 Antisense siRNA Decreased Spinal NL1 Expression

We then examined whether the lack of spinal NL1 modified SNL-induced allodynia by first implanting an intrathecal catheter to dispense drugs. After recovering from catheter implantation (3 days), the animals were administered an antisense siRNA that targeted NL1 (fig. 4A; it+NL1 RNAi), a missense siRNA (it+MS), or polyethylenimine (it+PEI, a transfection reagent) *via* the intrathecal catheter (daily for 4 days). Compared with the baseline level in naive animals (naive, 11.0 ± 1.61, n = 6), the implantation of an intrathecal catheter (it, 11.4 ± 2.33, n = 6) or the spinal administration of polyethylenimine (it+PEI, 10.4 ± 1.73, n = 6) or missense siRNA (it+MS 10 μg, 10 μl, 11.1 ± 2.13, n = 6) failed to affect NL1 expression in the dorsal horn. However, the NL1 mRNA-targeted siRNA (it+NL1 RNAi; 1, 5, and 10 μg; 10 μl) significantly reduced the spinal NL1 expression by decreasing the band intensity of NL1 in a dose-dependent manner (10.9 ± 2.41, 7.7 ± 1.63, and 4.87 ± 2.11 for 1, 5, and 10 μg, respectively, N = 6), which implies that our treatment sufficiently decreased NL1 expression in the spinal cord. To exclude the possibility of aberrant motor responses caused by the antisense administration, the motor abilities of the animals were assessed using the rota-rod test. The performance time of the rota-rod test did not significantly differ between the naive and polyethylenimine-treated (it+PEI), missense siRNA-treated (it+MS; 10 μg, 10 μl), or NL1 antisense siRNA-treated (it+NL1 RNAi; 10 μg, 10 μl) animals (fig. 4B; naive, 104.4 ± 13.50, 112.2 ± 21.0, 104.4 ± 19.49, 110.8 ± 24.83, and 106.9 ± 29.71; it+PEI, 112.4 ± 24.15, 106.4 ± 26.36, 108.9 ± 22.36, 104.7 ± 22.72, and 111.9 ± 21.11; it+MS, 104.4 ± 18.55, 103.9 ± 29.24, 101.8 ± 26.13, 104.6 ± 18.63, and 102.6 ± 20.68; it+NL1 RNAi, 108.0 ± 39.67, 102.8 ± 22.71, 116.0 ± 28.63, 112.8 ± 23.54, and 106.2 ± 24.82 at days 0, 1, 2, 3, and 4, respectively, all n = 10), indicating that our knockdown procedures did not induce motor deficits in animals.

NL1 Knockdown Prevented SNL-associated Allodynia

We next examined the effect of the NL1 knockdown on SNL-induced allodynia and observed that, although the paw withdrawal threshold of the sham-operated animals was not affected at any of the time points (fig. 4C; sham, 15.0 ± 0.00, 14.5 ± 1.58, 14.4 ± 4.90, 15.1 ± 4.36, and 15.6 ± 3.98; sham+it, 15.0 ± 0.00, 14.5 ± 1.58, 15.5 ± 6.13, 15.5 ± 6.13, and 15.7 ± 5.89; sham+it+MS, 15.0 ± 0.00, 14.5 ± 1.58, 15.5 ± 6.13, 15.5 ± 6.13, and 15.7 ± 5.89; sham+it+NL1 RNAi, 15.0 ± 0.00, 14.6 ± 4.64, 14.0 ± 2.11, 15.8 ± 7.32, and 16.1 ± 7.26 at days −1, 1, 3, 5, and 7, respectively, all n = 10), the spinal administration of NL1 antisense siRNA (fig. 4D; SNL+it+NL1 RNAi; 10 μg, 10 μl), but not missense siRNA (SNL+it+MS; 10 μg, 10 μl) or catheter implantation alone (SNL+it), partially prevented SNL-induced allodynia, as evidenced by the significant increases in the paw withdrawal thresholds 5 and 7 days after surgery (SNL, 15.0 ± 0.00, 5.4 ± 2.12, 1.1 ± 0.66, 1.6 ± 1.06, and 1.0 ± 1.29; SNL+it, 15.0 ± 0.00, 4.5 ± 2.48, 10.58 ± 0.49, 0.7 ± 0.56, and 0.55 ± 0.52; SNL+it+MS, 15.0 ± 0.00, 3.4 ± 2.34, 0.8 ± 0.83, 1.3 ± 1.21, and 0.9 ± 0.65; SNL+it+NL1 RNAi, 15.0 ± 0.00, 5.5 ± 2.89, 1.4 ± 0.74, 6.5 ± 3.37, and 8.4 ± 4.17 at days −1, 1, 3, 5, and 7, respectively, n = 10). These data provide genetic basis to support the role of spinal NL1 in SNL-induced allodynia.

NL1 Knockdown Attenuated SNL-induced NL1–PSD-95–pNR2B Interactions and NR2B Phosphorylation

We then investigated the possibility that the focal knockdown of spinal NL1 expression ameliorated allodynia by influencing the SNL-associated spinal NL1, PSD-95, and pNR2B interactions. In the PSD-95 and tNR2B precipitates (fig. 5, A–D; IP:PSD-95 and IP:tNR2B, respectively), NL1 antisense siRNA (SNL 7D+NL1 RNAi), but not the missense siRNA (SNL 7D+MS), reduced the SNL-enhanced abundances of PSD-95-bound NL1 and pNR2B (PSD-95/NL1, 11.9 ± 1.79 in sham 7D, 22.2 ± 2.81 in SNL 7D, 22.8 ± 2.40 in SNL 7D+MS, 16.0 ± 2.39 in SNL 7D+NL1 RNAi, n = 6; PSD-95/pNR2B, 11.2 ± 1.74 in sham 7D,

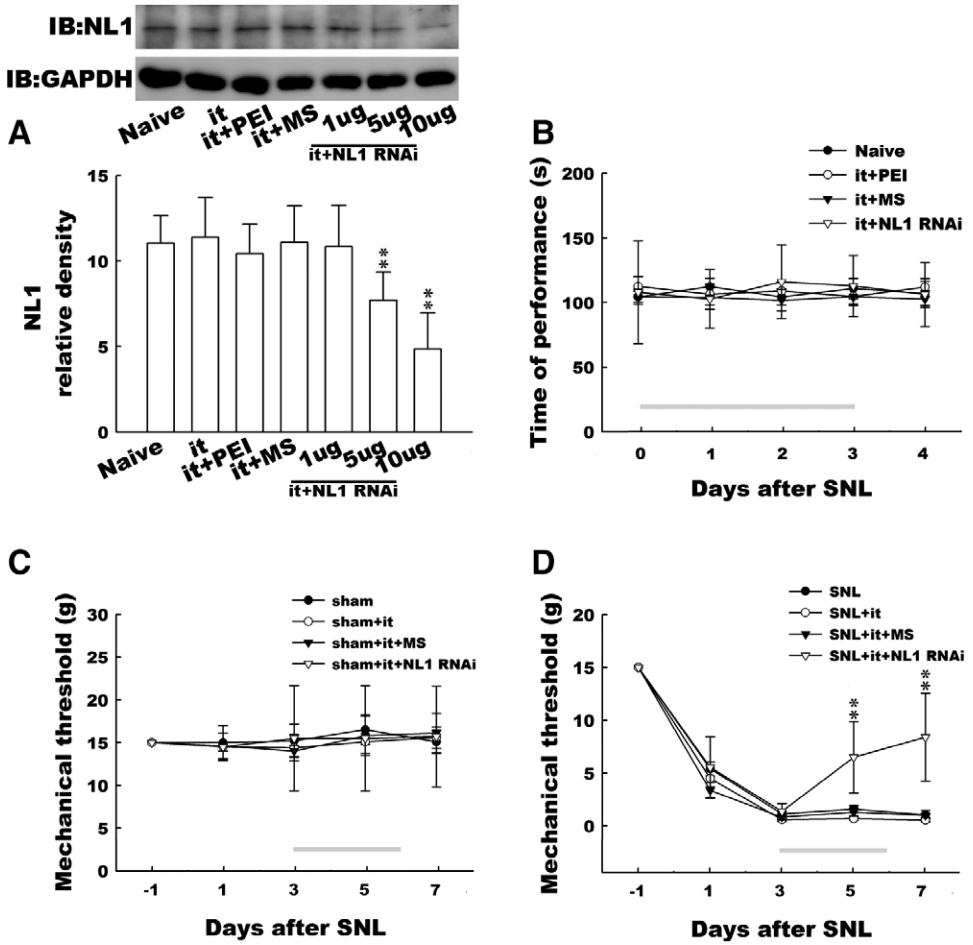

Fig. 4. Neuroligin-1 (NL1) knockdown prevents nerve ligation–induced behavioral allodynia. (*A*) The administration of an NL1 mRNA-targeting small-interfering RNA (siRNA, it+NL1 RNAi; 1, 5, and 10 μg; 10 μl) but not intrathecal catheter implantation (it), the administration of polyethylenimine (it+PEI, a transfection reagent, 10 μl), or missense siRNA (it+MS, 10 μg, 10 μl), dose dependently decreased the level of NL1 in the ipsilateral dorsal horn (**$P < 0.01$ *vs.* naive, n = 6). The level of glyceraldehyde 3-phosphate dehydrogenase (GAPDH) was used as a loading control. (*B*) The administration of polyethylenimine, missense siRNA, and NL1 mRNA-targeting siRNA (10 μg, 10 μl) failed to affect the performance times on the rota-rod test on days 0, 1, 2, 3, or 4 after treatment compared with the naive animals. (*C* and *D*) Although the treatments failed to produce effects in the sham-operated animals, NL1 mRNA-targeting siRNA (SNL+it+NL1 RNAi, 10 μg, 10 μl) significantly increased the withdrawal threshold in the spinal nerve ligation (SNL) animals at days 5 and 7 postsurgery (**$P < 0.01$ *vs.* SNL, n = 10). The *gray bar* at the bottom indicates the duration of administration. IB = immunoblot.

22.6 ± 2.67 in SNL 7D, 23.7 ± 2.40 in SNL 7D+MS, 18.6 ± 2.05 in SNL 7D+NL1 RNAi, n = 6) as well as those of the tNR2B-bound NL1, PSD-95, and pNR2B compared with the SNL group (SNL; tNR2B/NL1, 10.4 ± 1.54 in sham 7D, 16.9 ± 2.19 in SNL 7D, 17.5 ± 1.94 in SNL 7D+MS, 12.8 ± 1.51 in SNL 7D+NL1 RNAi, n = 6; tNR2B/PSD-95, 11.9 ± 1.62 in sham 7D, 19.7 ± 2.77 in SNL 7D, 19.3 ± 2.57 in SNL 7D+MS, 15.3 ± 1.87 in SNL 7D+NL1 RNAi, n = 6; tNR2B/pNR2B, 11.4 ± 2.61 in sham 7D, 22.1 ± 2.56 in SNL 7D, 21.3 ± 2.94 in SNL 7D+MS, 14.1 ± 2.29 in SNL 7D+NL1 RNAi, n = 6). In contrast, the PSD-95 and tNR2B immunoreactivities were similar across groups in the PSD-95 and tNR2B precipitates, respectively (PSD-95/PSD-95, 13.9 ± 1.91 in sham 7D, 12.9 ± 1.68 in SNL 7D, 13.8 ± 1.71 in SNL 7D+MS, 12.5 ± 1.74 in SNL 7D+NL1 RNAi, n = 6; tNR2B/tNR2B, 20.9 ± 2.28 in sham 7D, 21.1 ± 2.30 in SNL 7D, 20.5 ± 2.47 in SNL 7D+MS, 20.2 ± 2.80 in SNL 7D+NL1 RNAi, n = 6). These results suggest that spinal NL1 acts as an upstream factor in the SNL-provoked spinal interactions between NL1, PSD-95, and pNR2B. To confirm the effects of NL1 knockdown on the SNL-induced NL1, PSD-95, and pNR2B interactions and NR2B phosphorylation, the cellular expressions and locations of these candidate proteins after the daily administration of specific antisense siRNA were analyzed. Although we observed no effects on the immunofluorescence of PSD-95, the application of NL1 antisense siRNA (fig. 5E; SNL+NL1 RNAi) markedly reduced the NL1 and SNL-enhanced pNR2B and colocalized NL1–PSD-95–pNR2B immunofluorescence, as evidenced by the significant decreases in the NL1-positive, pNR2B-positive, and NL1–PSD-95–pNR2B triple-labeled neuron counts in the spinal slices compared with the SNL

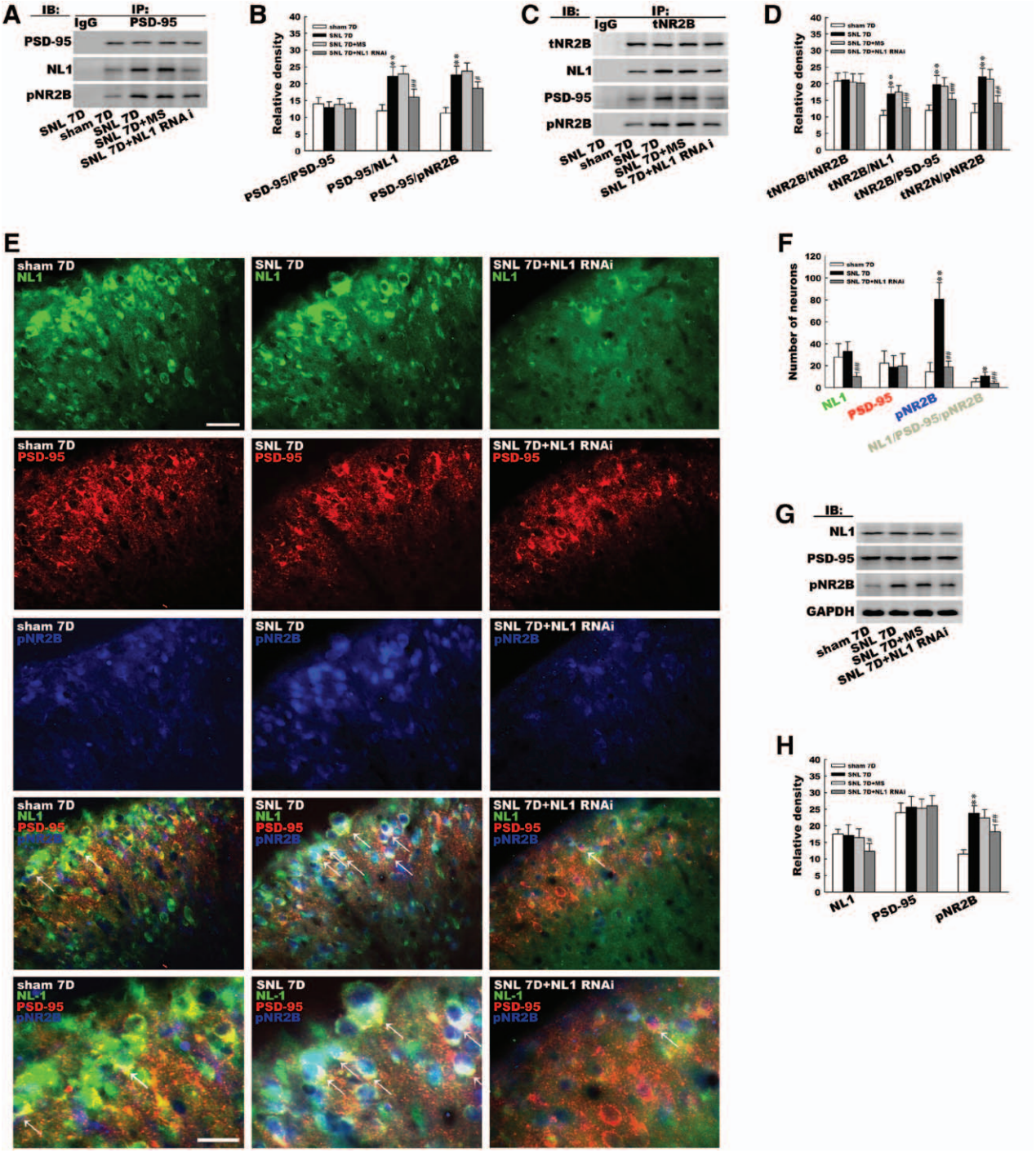

Fig. 5. Spinal nerve ligation (SNL) induces spinal neuroligin-1 (NL1)/postsynaptic density-95 (PSD-95)/phosphorylated NR2B (pNR2B) cascade-dependent NR2B phosphorylation. (*A*) The SNL (SNL 7D)-enhanced abundances of PSD-95-bound NL1 and pNR2B on day 7 in response to the spinal administration of NL1 mRNA-targeting small-interfering RNA (siRNA, SNL 7D+NL1 RNAi, 10 μg, 10 μl). No immunoreactivity for the candidate proteins was detected in the immunoglobulin G (IgG)-recognized precipitates. The PSD-95-recognized immunoprecipitates (IP) purified from the sham-operated (sham 7D) or SNL animals were immunoblotted (IB) for PSD-95, NL1, and pNR2B. (*B*) The NL1 mRNA-targeting siRNA reversed the SNL-induced increases in PSD-95–NL1 and PSD-95–pNR2B coprecipitation (**$P < 0.01$ *vs.* sham 7D, n = 6; #$P < 0.05$, ##$P < 0.01$ *vs.* SNL 7D, n = 6). (*C*) The SNL-induced enhancements in the abundances of total NR2B (tNR2B)-bound NL1, PSD-95, and pNR2B at day 7 in response to the spinal administration of NL1 mRNA-targeting siRNA. No immunoreactivity for the candidate proteins was detected in the IgG-recognized precipitates. (*D*) The NL1 mRNA-targeting siRNA reversed the SNL-induces increases in tNR2B–NL1, tNR2B–PSD-95, and tNR2B–pNR2B coprecipitation (**$P < 0.01$ *vs.* sham 7D, n = 6; ##$P < 0.01$ *vs.* SNL 7D, n = 6). (*E*) Although it elicited no effect on NL1 (*green*) or PSD-95 (*red*), SNL but not the sham operation notably enhanced the immunofluorescence of pNR2B (*blue*) in the

rats (fig. 5F; NL1, 27.8 ± 12.17 in sham 7D, 33.0 ± 8.92 in SNL 7D, 10.0 ± 3.69 in SNL 7D+NL1 RNAi, n = 6; PSD-95, 22.2 ± 11.3 in sham 7D, 18.8 ± 10.30 in SNL 7D, 19.7 ± 11.18 in SNL 7D+NL1 RNAi, n = 6; pNR2B, 14.5 ± 8.26 in sham 7D, 80.7 ± 15.08 in SNL 7D, 18.8 ± 5.38 in SNL 7D+NL1 RNAi, n = 6; NL1–PSD-95–pNR2B, 5.3 ± 3.01 in sham 7D, 10.5 ± 3.67 in SNL 7D, 3.8 ± 2.32 in SNL 7D+NL1 RNAi, n = 6). Moreover, although it did not affect the abundance of PSD-95 (fig. 5, G and H), the NL1 antisense siRNA, but not the missense RNA (SNL 7D+MS; 10 μg, 10 μl), markedly decreased the spinal NL1 expression and SNL-enhanced NR2B phosphorylation, as evidenced by the significant decreases in the band intensities of NL1 and pNR2B compared with the SNL group (SNL 7D; NL1, 17.6 ± 1.46 in sham 7D, 17.1 ± 3.24 in SNL 7D, 16.4 ± 2.70 in SNL 7D+MS, 12.3 ± 2.39 in SNL 7D+NL1 RNAi, n = 6; PSD-95, 23.9 ± 2.97 in sham 7D, 25.6 ± 3.26 in SNL 7D, 25.3 ± 2.83 in SNL 7D+MS, 26.0 ± 3.06 in SNL 7D+NL1 RNAi, n = 6; pNR2B, 11.5 ± 1.33 in sham 7D, 23.8 ± 2.27 in SNL 7D, 22.3 ± 2.58 in SNL 7D+MS, 18.1 ± 2.16 in SNL 7D+NL1 RNAi, n = 6). This result suggests that NL1 contributes to the development of allodynia, possibly by affecting the downstream interactions of spinal NL1, PSD-95, and pNR2B and NR2B phosphorylation.

Ro 25-6981 Ameliorated Allodynia by Antagonizing the Spinal PSD-95–pNR2B Interactions and NR2B Phosphorylation

To confirm the role of NR2B phosphorylation in the SNL-associated nociceptive hypersensitivity, we spinally injected Ro 25-6981, a selective NR2B antagonist, into rats at 7 days after SNL. The administration of Ro 25-6981 (fig. 6A; SNL 7D+Ro 25-6981; 30, 100, and 300 nM; 10 μl) but not the vehicle solution (SNL 7D+Veh) dose-dependently decreased the paw withdrawal thresholds from 1 to 8 h after injection compared with the SNL animals (SNL 7D; SNL 7D, 0.9 ± 1.18, 0.4 ± 0.29, 0.7 ± 0.44, 0.6 ± 0.44, 0.7 ± 0.53, 0.6 ± 0.40, 0.5 ± 0.46, 0.3 ± 0.37, and 0.5 ± 0.42; SNL 7D+Veh, 0.8 ± 0.44, 0.9 ± 0.77, 0.6 ± 0.43, 1.2 ± 0.78, 0.7 ± 0.80, 0.9 ± 0.58, 0.8 ± 0.44, 0.8 ± 0.69, and 0.8 ± 0.64; SNL 7D+Ro 25-6981 30 nM, 0.6 ± 0.48, 0.8 ± 0.63, 1.6 ± 1.02, 3.8 ± 2.1, 3.2 ± 1.83, 1.0 ± 0.58, 0.8 ± 0.53, 0.7 ± 0.45, and 0.9 ± 0.58; SNL 7D+Ro 25-6981 100 nM, 0.8 ± 0.56, 1.9 ± 1.77, 4.4 ± 2.07, 4.5 ± 2.27, 4.6 ± 1.90, 4.1 ± 2.46, 2.1 ± 1.05, 0.7 ± 0.42, and 0.8 ± 0.51; SNL 7D+Ro 25-6981 300 nM, 1.1 ± 0.79, 3.0 ± 1.27, 7.0 ± 2.16, 8.8 ± 1.40, 7.1 ± 3.90, 6.3 ± 3.27, 3.7 ± 3.12, 2.1 ± 1.05, and 2.1 ± 1.40 at hours 0, 1, 2, 3, 4, 5, 6, 7, and 8, respectively, all n = 10). However, the spinal injection of neither Ro 25-6981 (100 nM, 10 μl) nor the vehicle solution affected the paw withdrawal threshold of the sham-operated group measured at the identical time points (fig. 6B; sham 7D, 15.1 ± 4.36, 15.0 ± 6.38, 13.9 ± 5.09, 14.3 ± 6.75, 13.7 ± 5.29, 13.4 ± 5.21, 14.8 ± 6.58, 13.2 ± 5.39, and 13.9 ± 5.09; sham 7D+Veh, 14.0 ± 2.11, 15.6 ± 7.52, 15.0 ± 6.38, 13.6 ± 5.02, 14.1 ± 4.86, 14.3 ± 6.75, 15.0 ± 6.38, 14.2 ± 5.14, and 14.6 ± 6.77; sham 7D+Ro 25-6981 300 nM, 15.4 ± 4.32, 16.0 ± 5.83, 14.5 ± 1.58, 14.1 ± 4.89, 14.1 ± 4.86, 14.1 ± 4.86, 13.7 ± 6.66, 13.7 ± 5.29, and 14.9 ± 4.65 at hours 0, 1, 2, 3, 4, 5, 6, 7, and 8, respectively, all n = 10). When examining the PSD-95 precipitation, we found that Ro 25-6981 did not affect PSD-95 or the SNL-enhanced NL1 immunoreactivity (fig. 6, C and D; both compared with SNL 7D), but it markedly decreased the SNL-enhanced quantities of PSD-95-bound pNR2B (compared with SNL 7D) in the PSD-95 precipitates (IP:PSD-95; PSD-95/PSD-95, 16.7 ± 1.04 in sham 7D, 17.2 ± 1.81 in SNL 7D, 15.8 ± 1.43 in SNL 7D+Veh, 17.6 ± 0.97 in SNL 7D+Ro 25-6981, n = 6; PSD-95/NL1, 15.1 ± 1.51 in sham 7D, 23.3 ± 2.62 in SNL 7D, 22.8 ± 2.40 in SNL 7D+Veh, 21.9 ± 2.19 in SNL 7D+Ro 25-6981, n = 6; PSD-95/pNR2B, 13.2 ± 1.60 in sham 7D, 18.7 ± 1.81 in SNL 7D, 18.9 ± 2.20 in SNL 7D+Veh, 14.7 ± 2.36 in SNL 7D+Ro 25-6981, n = 6). These results suggest that neuropathic injury induced behavioral allodynia *via* spinal NL1/PSD-95/pNR2B cascade-dependent NR2B phosphorylation.

The Neurexin-1β Fc Antagonized SNL-associated Allodynia

A recombinant neurexin-1β Fc chimera fusion protein (Nrx1b Fc) has been shown to interfere with the binding of Nrx1b to NL, which affects the assembly of postsynaptic proteins that are crucial for NMDA-associated neurotransmission.[23] Therefore, we tested whether the spinal administration of the Nrx1b Fc could ameliorate neuropathic injury-induced allodynia. Seven days after surgery,

Fig. 5. (*Continued*). ipsilateral dorsal horn at day 7 postsurgery. pNR2B fluorescence costained with NL1 and PSD-95 in all groups (*white*, indicated by *arrows*). Spinal administration of NL1 mRNA-targeting siRNA reduced NL1 and the SNL-induced enhancement of pNR2B fluorescence and NL1–PSD-95–pNR2B costaining in the dorsal horn, but it failed to affect the immunofluorescence of PSD-95. Each of these images is representative of six sample preparations. *Scale bar* = 50 μm, thickness = 50 μm. (*F*) Although it elicited no effect NL1- or PSD-95-positive neurons, SNL significantly increased the pNR2B-positive and NL1/PSD-95/pNR2B triple-labeled neuron counts (**P* < 0.05, ***P* < 0.01 *vs.* sham 7D, n = 6). In addition to decreasing the number of NL1-positive neurons, the spinal administration of NL1 mRNA-targeting siRNA significantly decreased the SNL-induced increases in the counts of pNR2B-positive and NL1/PSD-95/pNR2B triple-labeled neurons (##*P* < 0.01 *vs.* SNL 7D, n = 6). (*G*) The abundances of NL1, PSD-95, and pNR2B at day 7 after SNL in response to the spinal administration of NL1 mRNA-targeting siRNA. The level of glyceraldehyde 3-phosphate dehydrogenase protein (GAPDH) was used as a loading control. (*H*) The spinal administration of NL1 mRNA-targeting siRNA significantly decreased NL1 expression and the nerve ligation–induced enhancement of pNR2B expression the in dorsal horn samples, but both treatments failed to affect the level of PSD-95 (***P* < 0.01 *vs.* sham 7D, n = 6; #*P* < 0.05, ##*P* < 0.01 *vs.* SNL 7D, n = 6). 7D = day 7 postsurgery; MS = missense.

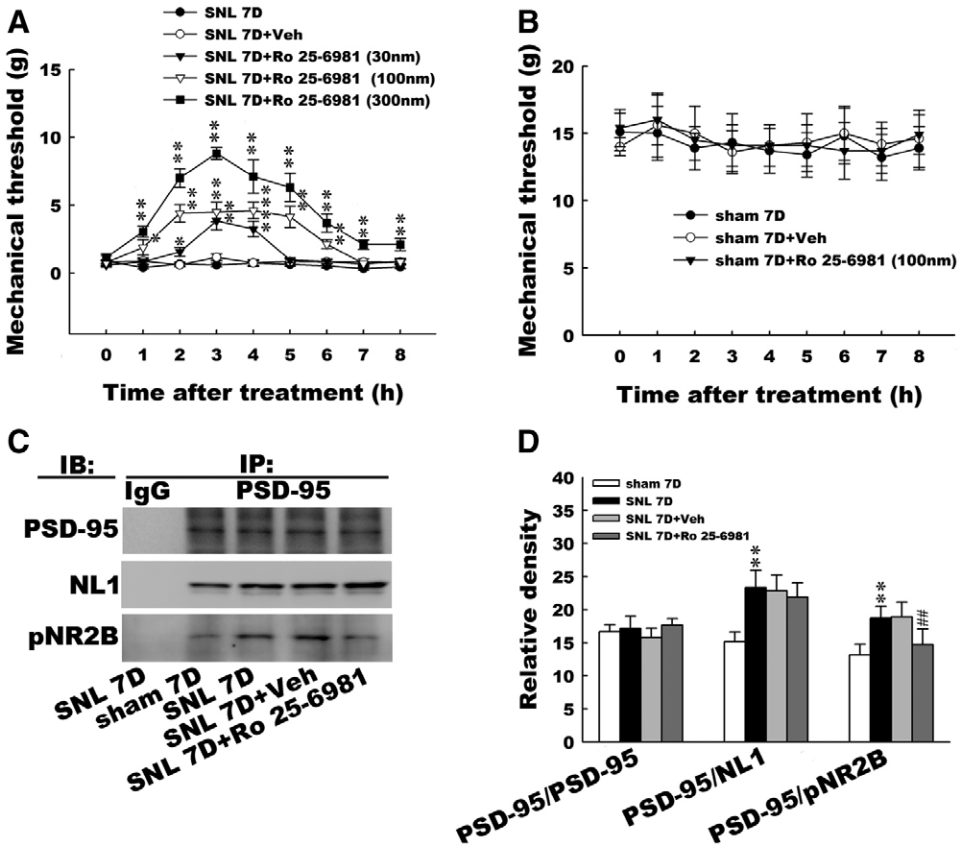

Fig. 6. Ro 25-6981 reversed spinal nerve ligation (SNL)–induced allodynia and spinal neuroligin-1 (NL1)/postsynaptic density-95 (PSD-95)/NR2B interaction. (*A*) At day 7 after SNL (SNL 7D), spinal administration with Ro 25-6981 (SNL 7D+Ro 25-6981; 30, 100, and 300 nM; 10 μl) but not the vehicle solution (SNL 7D+veh) increased the withdrawal threshold of the ipsilateral hind paw at hours 1 to 8 after treatment (*$P < 0.05$, **$P < 0.01$ *vs.* SNL 7D, n = 7). (*B*) At day 7 after the sham operation, neither Ro 25-6981 (Sham 7D+Ro 25-6981) nor the vehicle solution (Sham 7D+veh) affected the withdrawal threshold of the ipsilateral hind paw measured at hours 1 to 8 after treatment. (*C*) SNL-induced enhancements in the abundances of PSD-95-bound NL1 and phosphorylated NR2B (pNR2B) at day 7 in response to the spinal administration of Ro 25-6981. No immunoreactivity for the candidate proteins was detected in the immunoglobulin G (IgG)-recognized precipitates. (*D*) Although it elicited no effect on PSD-95-bound NL1, the spinal injection of Ro 25-6981 significantly decreased the SNL-induced enhancement in the abundance of PSD-95-bound pNR2B (**$P < 0.01$ *vs.* sham 7D; ##$P < 0.01$ *vs.* SNL 7D). IB = immunoblot; IP = immunoprecipitate.

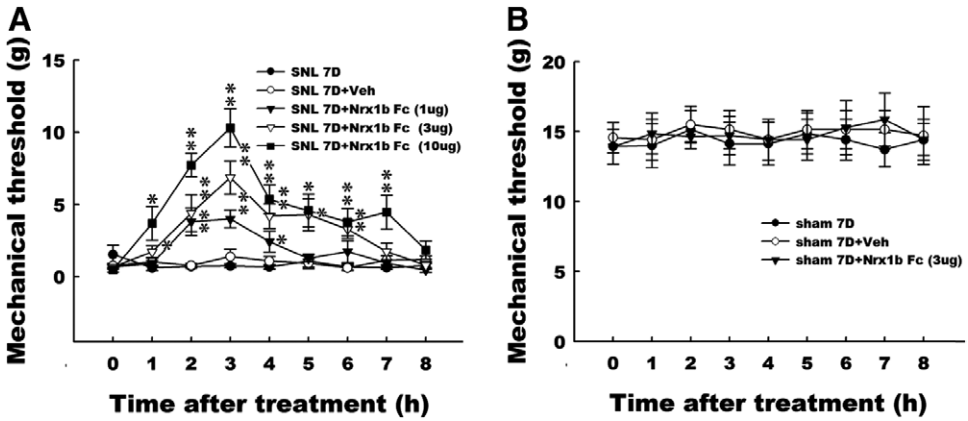

Fig. 7. Neurexin-1β chimera antagonizes nerve ligation–induced behavioral allodynia. (*A*) At day 7 after spinal nerve ligation (SNL; SNL 7D), administration with a recombinant neurexin-1β Fc chimera (Nrx1b Fc; 1, 3, and 10 μg; 10 μl; SNL 7D+Nrx1b Fc) but not the vehicle solution (SNL 7D+veh) increased the withdrawal threshold of the ipsilateral hind paw at hours 1 to 7 after treatment (*$P < 0.05$, **$P < 0.01$ *vs.* SNL 7D, n = 7). (*B*) At day 7 after sham operation (sham 7D), neither administration with an Nrx1b Fc (3 μg, 10 μl) nor the vehicle solution affected the withdrawal threshold tested at time points.

the intrathecal application of the Nrx1b Fc (fig. 7A; SNL 7D+Nrx1b Fc; 1, 3, and 10 μg; 10 μl), but not the vehicle solution (SNL 7D+Veh), ameliorated the SNL-induced behavioral allodynia, as evidenced by the dose-dependent decreases in the paw withdrawal thresholds from 1 to 7 h after injection compared with the SNL animals (SNL 7D; SNL 7D, 1.5 ± 1.70, 0.6 ± 0.45, 0.7 ± 0.31, 0.7 ± 0.34, 0.7 ± 0.41, 1.1 ± 1.33, 0.7 ± 0.52, 0.6 ± 0.30, and 0.8 ± 0.47; SNL 7D+Veh, 0.8 ± 0.40, 1.0 ± 0.81, 0.7 ± 0.37, 1.4 ± 1.34, 1.1 ± 0.82, 0.9 ± 0.71, 0.6 ± 0.45, 1.14 ± 0.80, and 1.2 ± 0.69; SNL 7D+Nrx1b Fc 1 μg, 0.7 ± 0.41, 0.9 ± 0.53, 3.8 ± 2.56, 4.0 ± 1.63, 2.4 ± 1.92, 1.3 ± 0.63, 1.7 ± 2.02, 0.9 ± 0.57, and 0.5 ± 0.41; SNL 7D+Nrx1b Fc 3 μg, 0.7 ± 0.37, 1.7 ± 1.16, 4.4 ± 3.38, 6.9 ± 3.02, 4.2 ± 2.25, 4.3 ± 2.93, 3.3 ± 1.70, 1.7 ± 1.55, and 0.8 ± 0.68; SNL 7D+Nrx1b Fc 5 μg, 0.5 ± 0.40, 3.7 ± 3.10, 7.7 ± 2.13, 10.2 ± 3.49, 5.3 ± 2.65, 4.6 ± 2.99, 3.7 ± 2.56, 4.5 ± 3.09, and 1.8 ± 1.66 at hours 0, 1, 2, 3, 4, 5, 6, 7, and 8, respectively, all n = 10). Nevertheless, the Nrx1b Fc did not affect the paw withdrawal thresholds of the sham-operated group measured at the same time points (fig. 7B; sham 7D, 13.9 ± 4.61, 14.0 ± 5.88, 15.1 ± 5.13, 14.1 ± 5.74, 14.1 ± 5.74, 14.8 ± 5.48, 14.4 ± 5.46, 13.7 ± 4.56, and 14.4 ± 5.46; sham 7D+Veh, 14.6 ± 4.09, 14.4 ± 5.46, 15.5 ± 4.91, 15.1 ± 5.12, 14.4 ± 5.46, 15.1 ± 5.12, 15.1 ± 5.12, 15.1 ± 5.12, and 14.7 ± 7.74; sham 7D++Nrx1b Fc, 13.9 ± 4.61, 14.9 ± 5.48, 14.6 ± 1.37, 14.7 ± 5.17, 14.4 ± 5.45, 14.4 ± 5.45, 15.3 ± 7.24, 15.9 ± 7.06, and 14.4 ± 4.29 at hours 0, 1, 2, 3, 4, 5, 6, 7, and 8, respectively, all n = 10). These results suggest that the Nrx1b Fc, which is presumed to interrupt Nrx1b–NL1 interactions, ameliorated SNL-induced behavioral allodynia.

The Nrx1b Fc Antagonized the Spinal NL1/PSD-95/pNR2B Interactions

Nrx1b–NL1 interactions have been demonstrated to play a key role in the glutamatergic receptor–dependent synaptic plasticity,[34] which is crucial for pain hypersensitivity.[17] Because Nrx1b Fc blocks NMDA synapse formation by impeding Nrx1b–NL1 interactions,[35] the analgesic effect of the Nrx1b Fc may be due to its effect on the spinal NL1/PSD-95/pNR2B cascade. This hypothesis was tested using immunohistochemical analyses. Although the PSD-95 immunoreactivities did not significantly differ between groups (fig. 8, A and B; PSD-95, 30.3 ± 7.66 in sham 7D, 29.0 ± 9.67 in SNL 7D, 31.8 ± 10.12 in SNL 7D+Nrx1b Fc, n = 6), the statistical analyses revealed that Nrx1b Fc reduced both the SNL-enhanced pNR2B and PSD-95/pNR2B-colocalized immunoreactivities, as evidenced by the significant decreases in the pNR2B-positive and PSD-95/pNR2B double-labeled neuron counts (pNR2B, 20.8 ± 8.51 in sham 7D, 84.3 ± 12.51 in SNL 7D, 24.7 ± 11.7 in SNL 7D+Nrx1b Fc, n = 6; PSD-95/pNR2B, 9.6 ± 3.77 in sham 7D, 19.3 ± 8.55 in SNL 7D, 7.2 ± 3.76 in SNL 7D+Nrx1b Fc, n = 6). We next examined the effects of Nrx1b Fc on the expressions of candidate proteins using Western blotting. Without affecting the abundances of Nrx1b, NL1, or PSD-95 (fig. 8, C and D; Nrx1b, 13.8 ± 2.59 in sham 7D, 12.5 ± 2.71 in SNL 7D, 13.3 ± 2.34 in SNL 7D+Veh, 13.0 ± 2.74 in SNL 7D+Nrx1b Fc, n = 6; NL1, 16.8 ± 3.19 in sham 7D, 18.0 ± 2.22 in SNL 7D, 18.8 ± 1.95 in SNL 7D+Veh, 17.2 ± 1.43 in SNL 7D+Nrx1b Fc, n = 6; PSD-95, 27.4 ± 3.80 in sham 7D, 26.6 ± 3.70 in SNL 7D, 26.6 ± 3.70 in SNL 7D+Veh, 26.8 ± 4.04 in SNL 7D+Nrx1b Fc, n = 6), the administration of Nrx1b Fc significantly reversed the SNL-induced NR2B phosphorylation, as evidenced by a decrease in the pNR2B band intensity compared with the SNL group (pNR2B, 15.3 ± 2.82 in sham 7D, 23.9 ± 3.03 in SNL 7D, 23.2 ± 3.01 in SNL 7D+Veh, 16.4 ± 2.94 in SNL 7D+Nrx1b Fc, n = 6). These results suggest that the spinal application of Nrx1b Fc attenuated SNL-enhanced PSD-95/pNR2B-dependent NR2B phosphorylation. The coprecipitation experiments showed that although the PSD-95 and tNR2B immunoreactivities did not differ between groups in the PSD-95 (fig. 8, E and F; IP:PSD-95) and tNR2B (fig. 8, G and H; IP:tNR2B) precipitates (PSD-95/PSD-95, 17.8 ± 1.88 in sham 7D, 17.3 ± 2.00 in SNL 7D, 17.9 ± 2.30 in SNL 7D+Veh, 16.8 ± 1.48 in SNL 7D+Nrx1b Fc, n = 6; tNR2B/tNR2B, 22.2 ± 2.30 in sham 7D, 22.6 ± 1.75 in SNL 7D, 21.7 ± 1.14 in SNL 7D+Veh, 21.4 ± 1.74 in SNL 7D+Nrx1b Fc, n = 6), the intrathecal administration of Nrx1b Fc (SNL 7D+Nrx1b Fc; 10 μg, 10 μl) significantly decreased the SNL-enhanced abundances of PSD-95-bound NL1 and pNR2B (PSD-95/NL1, 9.6 ± 2.51 in sham 7D, 17.5 ± 1.93 in SNL 7D, 16.6 ± 2.53 in SNL 7D+Veh, 11.4 ± 1.43 in SNL 7D+Nrx1b Fc, n = 6; PSD-95/pNR2B, 12.2 ± 2.35 in sham 7D, 20.6 ± 2.71 in SNL 7D, 21.9 ± 2.65 in SNL 7D+Veh, 12.9 ± 2.15 in SNL 7D+Nrx1b Fc, n = 6) and that of tNR2B-bound NL1, PSD-95, and pNR2B (tNR2B/NL1, 11.0 ± 1.78 in sham 7D, 19.8 ± 2.48 in SNL 7D, 18.6 ± 1.78 in SNL 7D+Veh, 11.6 ± 1.88 in SNL 7D+Nrx1b Fc, n = 6 tNR2B/PSD-95, 13.1 ± 2.93 in sham 7D, 21.3 ± 3.01 in SNL 7D, 20.4 ± 2.41 in SNL 7D+Veh, 16.7 ± 3.04 in SNL 7D+Nrx1b Fc, n = 6; tNR2B/pNR2B, 13.5 ± 2.05 in sham 7D, 23.6 ± 2.01 in SNL 7D, 25.2 ± 2.33 in SNL 7D+Veh, 16.5 ± 2.18 in SNL 7D+Nrx1b Fc, n = 6). This effect was not observed for the vehicle solution (SNL 7D+Veh). Taken together, these results suggest that the analgesic effects of NRX1β Fc could be attributed to the interruption of SNL-induced spinal Nrx1b–NL1 interactions and subsequent NL1/PSD-95/pNR2B cascade-dependent NR2B phosphorylation.

Discussion

In the current study, we found that experimental neuropathic injury provoked the interaction of NL1 and PSD-95, which subsequently enhanced the PSD-95–NR2B coupling–dependent NR2B phosphorylation in dorsal horn neurons that underlie the nociceptive hypersensitivity in rats. Moreover, the pharmacological perturbation of the transsynaptic Nrx1b–NL1 interactions using a recombinant Nrx1b Fc prevented neuropathic allodynia, possibly by abolishing the spinal NL1/PSD-95/pNR2B cascade (fig. 9).

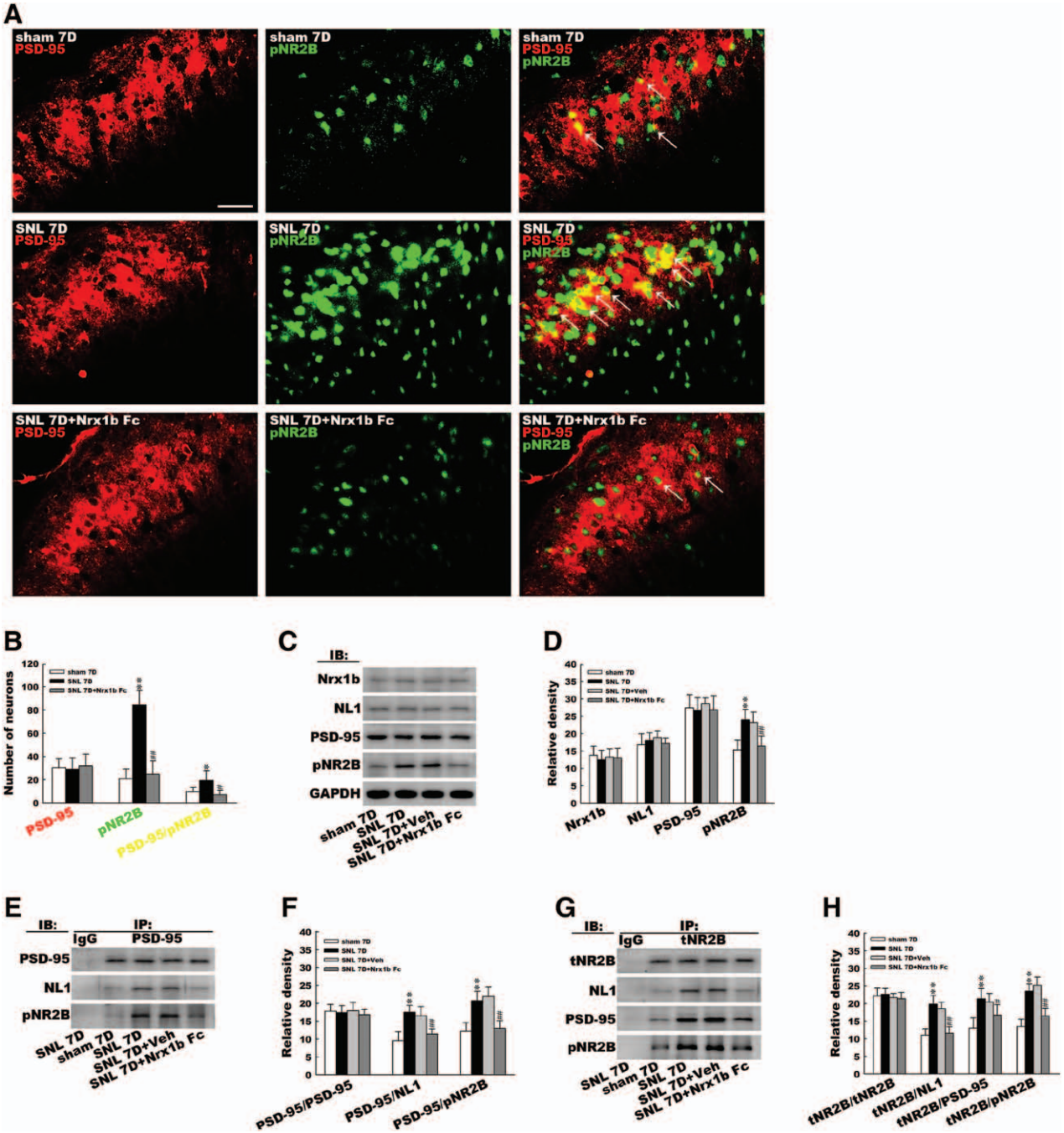

Fig. 8. Neurexin-1β chimera prevents nerve ligation–induced protein interactions and NR2B phosphorylation. (*A*) When compared with the sham operation (sham 7D), although spinal nerve ligation (SNL; SNL 7D) exhibited no effect on the postsynaptic density-95 (PSD-95) immunofluorescence (*red*), it notably enhanced the phosphorylated NR2B (pNR2B) immunofluorescence (*green*) in the ipsilateral dorsal horn at day 7 postsurgery (7D). The pNR2B fluorescence costained with PSD-95 (*yellow*, indicated by *arrows*); the nerve ligation–enhanced pNR2B immunoreactivity and pNR2B–PSD-95 costaining in the ipsilateral dorsal horn were both markedly reduced by the administration with a neurexin-1β Fc chimera (Nrx1b Fc), though this treatment did not affect the PSD-95 fluorescence (SNL 7D+Nrx1b Fc, 3 μg, 10 μl). Each of these immunofluorescence images is a representative of six sample preparations. *Scale bar* = 50 μm, thickness = 50 μm. (*B*) Administration with an Nrx1b Fc significantly reversed the SNL-increased counts of pNR2B-positive and PSD-95/pNR2B colabeled neurons (*$P < 0.05$, **$P < 0.01$ *vs.* sham 7D, n = 6; #$P < 0.05$, ##$P < 0.01$ *vs.* SNL 7D, n = 6). (*C*) The abundances of neurexin-1β (Nrx1b), neuroligin-1 (NL1), PSD-95, and pNR2B at day 7 after SNL (SNL 7D) in response to spinal administration with an Nrx1b Fc (SNL 7D+Nrx1b Fc, 3 μg, 10 μl). The level of glyceraldehyde 3-phosphate dehydrogenase proteins (GAPDH) was used as a loading control. (*D*) Without affecting the levels of Nrx1b, NL1, or PSD-95, spinal administration with Nrx1b Fc (**$P < 0.01$ *vs.* sham 7D, n = 6; ##$P < 0.01$ *vs.* SNL 7D, n = 7), but not the vehicle (Veh) solution ($P > 0.05$ *vs.* SNL 7D, n = 7), significantly decreased the SNL-enhanced pNR2B band intensity.

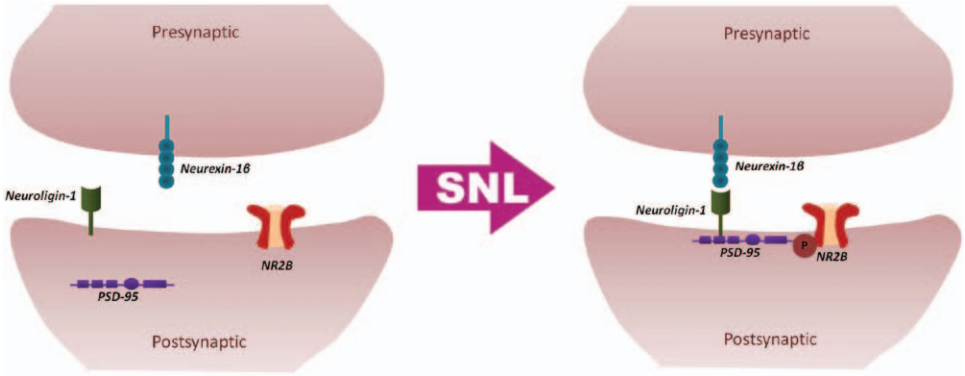

Fig. 9. Schematic diagram showing spinal neurexin-1β–neuroligin 1 interaction–dependent plasticity caused by neuropathic injury. Spinal nerve ligation (SNL) could provoke a transsynaptic interaction between the neurexin-1β and neuroligin-1, which associates with postsynaptic density-95 (PSD-95) to enhance the PSD-95–NR2B coupling–dependent NR2B phosphorylation in dorsal horn neurons.

Neuroligin-1 has recently been proposed to participate in memory consolidation because NL1 knockout mice display altered spatial learning and memory.[5] Using transgenic animals, Dahlhaus *et al.*[36] demonstrated that NL1 overexpression alters synaptic excitability in the hippocampus and that such alterations are accompanied by modified memory acquisition. Moreover, NL1 has been shown to be necessary for the expression of LTP in the amygdala that underlies associative fear memory,[6] and NL1 knockout rats display significant impairments in evoked LTP in the amygdala.[13] Together, these studies suggest that NL1 crucially contributes to learning-/memory-associated neural plasticity. The C-terminal tails of NLs interact with PSD-95 *via* PSD-95/discs large/zona occludens-1–dependent interactions.[10] The coexpression of NL1 with PSD-95 in cultured neurons coordinates the maturation of postsynaptic elements that modify the excitation/inhibition ratio of the synapse.[24] The expression of a dominant-negative NL1 that interrupts the binding of NL1 to PSD-95 remarkably reduces the sizes and densities of PSD-95 puncta in primary hippocampal cultures, which confirms that the NL1–PSD-95 interaction is involved in postsynaptic functions.[23] Studies of spinal LTP, which is a possible mechanism of the central sensitization that underlies nociceptive hypersensitivity, have revealed that pain-related spinal plasticity shares many features with LTP in brain areas.[9] Consistent with a recent study demonstrating that neuropathic injury does not alter spinal NL1 expression,[37] we observed that the abundance of NL1 in the dorsal horn was not modified after SNL. Nevertheless, SNL induced behavioral allodynia that was accompanied by the physical coupling of NL1 and PSD-95 in the spinal cord. Moreover, the postinjury NL1 immunofluorescence coincided with NeuN immunofluorescence and was demonstrated to colocalize with the PSD-95 reactivity in the dorsal horn. These findings imply that the NL1–PSD-95 interaction in spinal neurons crucially contributes to the development of neuropathic allodynia. This conclusion was further supported by the finding that the focal knockdown of spinal NL1 expression, which reversed the decreased withdrawal threshold caused by neuropathic injury, attenuated the SNL-induced NL1–PSD-95 association in the dorsal horn samples. In parallel with studies that have linked NL1 to learning- and/or memory-related LTP in brain areas, our findings provide evidence that supports the role of NL1–PSD-95 interaction in the spinal neural plasticity that mediates pain hypersensitivity after neuropathic injury.

Studies investigating visceral pain have demonstrated that the acute irritation of the pelvic organs provokes NR2B phosphorylation in the lumbosacral dorsal horn.[14,16,32,38,39] The focal trim-down of spinal NR2B expression[14,40] or intrathecal application of reagents that selectively antagonize NR2B phosphorylation[14,32,38,39] ameliorated irritation-induced visceral hyper-reflexia, which suggests that the activation of the NR2B subunits of NMDARs in the dorsal horn neurons is vitally involved in pain pathology. Moreover, both the developments of visceral[14,41] and somatic pain[15,17] are associated with the physical coupling of PSD-95 to NR2B and the subsequent NR2B phosphorylation in the spinal cord. Our previous study has shown that SNL time-dependently

Fig. 8. (*Continued*). (*E*) SNL-enhanced abundances of PSD-95-bound NL1 and pNR2B at day 7 in response to spinal administration with an Nrx1b Fc (SNL 7D+Nrx1b Fc, 3 μg, 10 μl). No immunoreactivity of candidate proteins was detected in the immunoglobulin G (IgG)-recognized precipitates. (*F*) Spinal injection of a neurexin-1β chimera (SNL 7D+Nrx1b Fc, 3 μg, 10 μl) significantly decreased the nerve ligation–enhanced abundance of PSD-95-bound NL1 and pNR2B (***P* < 0.01 *vs.* sham 7D; ##*P* < 0.01 *vs.* SNL 7D). (*G*) SNL-enhanced abundances of total NR2B (tNR2B)-bound NL1 and pNR2B at day 7 in response to spinal administration with an Nrx1b Fc (SNL 7D+Nrx1b Fc, 3 μg, 10 μl). No immunoreactivity of candidate proteins was detected in the IgG-recognized precipitates. (*H*) Spinal injection of Nrx1b Fc (SNL 7D+Nrx1b Fc, 3 μg, 10 μl) significantly decreased the nerve ligation–enhanced abundance of tNR2B-bound NL1, PSD-95, and pNR2B (***P* < 0.01 *vs.* sham 7D; ##*P* < 0.01 *vs.* SNL 7D). IB = immunoblot; IP = immunoprecipitate.

provoked allodynia and pNR2B expression with a maximal effect at 7 days after surgery.[17] We examine dorsal horn NR2B phosphorylation at day 7 post-SNL. In agreement with these studies, our data demonstrated that neuropathic injury induced spinal NR2B phosphorylation, as evidenced by the up-regulation of pNR2B expression in the dorsal horn. In addition to enhancing the pNR2B immunofluorescence that was demonstrated to colocalize with PSD-95, neuropathic injury provoked PSD-95–pNR2B coupling in the dorsal horn. These results reveal that the spinal PSD-95–NR2B interactions and NR2B activation participate in the development of neuropathic pain. In addition, NL1 directly interacts with PSD-95 to organize the juxta-membrane intracellular domain of the postsynaptic NMDARs and thereby clusters NMDARs on the postsynaptic site[42] to modify the efficacy of NMDAR-mediated neurotransmission.[43] In the current study, the results obtained from the experiments using siRNAs demonstrated that the knockdown of spinal NL1 expression prevented the SNL-enhanced spinal NR2B phosphorylation, the NL1–PSD-95 and PSD-95–pNR2B interactions, and the NL1–PSD-95–pNR2B colocalization in the dorsal horn, which was accompanied by the amelioration of behavioral allodynia. Conversely, although the administration of the selective NR2B antagonist that prevented SNL-induced NR2B phosphorylation efficiently prevented the SNL-induced reductions in the withdrawal thresholds and spinal PSD-95–pNR2B coupling, it did not affect the SNL-enhanced NL1–PSD-95 coprecipitation. Together, these findings provide genetic and pharmacological evidence that supports the notion that PSD-95–NR2B coupling–dependent NR2B activation is a downstream target of spinal NL1–PSD-95 interactions during the development of neuropathic pain.

Neuroligin was first identified as one of the binding partners of neurexins (Nrx), which are presynaptic CAMs.[18,44] The extracellular domain of NL binds to that of Nrx in a calcium ion–dependent manner and thereby connects the synaptic cleft and links NL to the exocytotic machinery.[45,46] In Aplysia, the depletion of Nrx in the presynaptic sensory neuron or NL in the postsynaptic motor neuron abolishes the long-term facilitation of the gill-withdrawal reflex, which is a form of learned fear. However, the overexpression of either Nrx or NL alone does not induce long-lasting synaptic facilitation, which suggests that the coordinated increase and subsequent functional transsynaptic interactions of Nrx and NL are crucial for learning-related synaptic plasticity.[47] Emerging studies have revealed that splice site 4 of Nrx1 is a critical regulator of NL1–Nrx interactions.[25,48] Recombinant Nrx1b Fc that lacks an insertion in splice site 4 reduces the Nrx1b–NL1 interaction and thereby diminishes glutamatergic synapse assembly.[49] Because there is not yet an Nrx1b Fc that does not include the splice site 4 insertion commercially available for rats, a recombinant human Nrx1b Fc was administered to the rats to perturb the transsynaptic Nrx1b–NL1 interactions in the current study. Our procedure was based on the fact that the extracellular domain of this reagent shares 99% amino acid sequence identity with the rat Nrx1b and has been found to interact well with native NL in rats.[50] We found that the spinal administration of the Nrx1b chimera ameliorated neuropathic injury–associated nociceptive hypersensitivity. Our findings agree with studies that have demonstrated that the Nrx1b–NL interaction plays a key role in learning-/memory-related neural plasticity. To the best of our knowledge, our findings are also the first to show that the perturbation of spinal Nrx1b and NL1 coupling eradicated the neural plasticity underlying neuropathic pain development. Moreover, consistent with the studies that have shown that transsynaptic Nrx1b–NL1 interactions in hippocampal neurons induce NL1–PSD-95 clustering, which recruited NMDARs to the postsynaptic site,[22] our results demonstrated that the application of Nrx1b Fc attenuated the neuropathic injury–associated NL1–PSD-95 and PSD-95–pNR2B coprecipitations and PSD-95–pNR2B colocalization in the dorsal horn. These findings imply that the transsynaptic Nrx1b–NL1 interactions crucially regulate the assembly of postsynaptic NMDARs. Specifically, we observed that Nrx1b Fc abolished neuropathic injury–associated spinal NR2B phosphorylation. Our results further extend the role of transsynaptic Nrx1b–NL1 interactions in the postsynaptic NMDAR activation, which is a pivotal piece of machinery for the development of the neural plasticity that underlies memory consolidation and nociceptive hypersensitivity.

In the current study, we showed that the NL1–PSD-95 interaction participates in neuropathic allodynia development by activating a postsynaptic PSD-95/NR2B cascade. Nevertheless, in hippocampal pyramidal cells, the NL1/PSD-95 complex has been demonstrated to modulate the neurotransmitter release probability and consequently alter short-term plasticity *via* a retrograde transsynaptic protein–protein interaction with Nrx1b.[51] Therefore, further studies are warranted to determine whether NL1-dependent retrograde modulation also plays a role in pain pathology. In contrast, in addition to directly coupling with glutamatergic NMDAR, PSD-95 indirectly interacts with AMPAR by binding to the auxiliary subunit stargazin and the related transmembrane AMPAR-associated proteins.[52,53] An electrophysiological investigation of mouse hippocampal neurons demonstrated that Nrx1b–NL1 adhesions postsynaptically mobilize glutamatergic AMPARs *via* a PSD-95-dependent diffusion/trap process.[34] Because a study published by our laboratory demonstrated that spinal AMPAR trafficking participates in complete Freund's adjuvant–induced inflammatory pain,[28] the possibility that PSD-95-dependent AMPAR recycling is also a downstream target of NL1 during the mediation of pain development needs to be seriously considered.

The NL family has been described to execute several specialized functions: NL1 primarily localizes to excitatory synapses,[7] whereas NL2 localizes to inhibitory synapses.[25,54] In addition to the results in the current study that demonstrated that NL1–PSD-95 coupling in the dorsal horn plays a role

in neuropathic pain, Dolique *et al.*[37] have recently linked spinal NL2–PSD-95 interactions to neuropathic pain by showing that SNL up-regulated NL2 expression accompanied by NL2–PSD-95 coupling in the dorsal horn. Moreover, similar to our results, Dolique *et al.* also demonstrated that the abundance of spinal NL1 remains unchanged after SNL. Nevertheless, as we examined the participation of NLs in pain pathology by focusing only on NL1 in the current study, the potential contribution of synergistic/antagonistic actions between NL members to neuropathic pain, for example, the counter balance between NL1-facilitated excitatory synapses[55] and NL2-impeded inhibitory synapses on pain-associated spinal plasticity, requires further investigations.

Acknowledgments

This research was supported by the National Science Council, Taipei, Taiwan (grant nos. NSC 102-2628-B-715-001 and 101-2320-B-715-001-MY3 to Dr. Peng and NSC 101-2320-B-039-013-MY3 to Dr Lin), by the Ministry of Science and Technology, Taipei, Taiwan (grant no. MOST 104-2320-B-019-MY3); by the Mackay Memorial Hospital, Taipei, Taiwan (grant nos. MMH-MM-10206 and MMH-MM-10302 to Dr. Peng), by the Taipei Medical University, Taipei, Taiwan (grant no. TMU102-AE1-B06 to Dr. Lin), and by Saint Paul's Hospital, Taoyuan, Taiwan (grant no. SPMRD-U1-6003 to Dr. Lin).

Competing Interests

The authors declare no competing interests.

Correspondence

Address correspondence to Dr. Peng: Department of Medicine, Mackay Medical College, No. 46, Sec. 3, Zhongzheng Road, Sanzhi District, New Taipei, Taiwan 25245. hsien.yu@gmail.com. Information on purchasing reprints may be found at www.anesthesiology.org or on the masthead page at the beginning of this issue. Anesthesiology's articles are made freely accessible to all readers, for personal use only, 6 months from the cover date of the issue.

References

1. Siegelbaum SA, Kandel ER: Learning-related synaptic plasticity: LTP and LTD. Curr Opin Neurobiol 1991; 1:113–20
2. Thalhammer A, Cingolani LA: Cell adhesion and homeostatic synaptic plasticity. Neuropharmacology 2014; 78:23–30
3. Lisé MF, El-Husseini A: The neuroligin and neurexin families: From structure to function at the synapse. Cell Mol Life Sci 2006; 63:1833–49
4. Craig AM, Kang Y: Neurexin-neuroligin signaling in synapse development. Curr Opin Neurobiol 2007; 17:43–52
5. Blundell J, Blaiss CA, Etherton MR, Espinosa F, Tabuchi K, Walz C, Bolliger MF, Südhof TC, Powell CM: Neuroligin-1 deletion results in impaired spatial memory and increased repetitive behavior. J Neurosci 2010; 30:2115–29
6. Kim J, Jung SY, Lee YK, Park S, Choi JS, Lee CJ, Kim HS, Choi YB, Scheiffele P, Bailey CH, Kandel ER, Kim JH: Neuroligin-1 is required for normal expression of LTP and associative fear memory in the amygdala of adult animals. Proc Natl Acad Sci U S A 2008; 105:9087–92
7. Song JY, Ichtchenko K, Südhof TC, Brose N: Neuroligin 1 is a postsynaptic cell-adhesion molecule of excitatory synapses. Proc Natl Acad Sci U S A 1999; 96:1100–5
8. Shipman SL, Nicoll RA: A subtype-specific function for the extracellular domain of neuroligin 1 in hippocampal LTP. Neuron 2012; 76:309–16
9. Sharif-Naeini R, Basbaum AI: Targeting pain where it resides. In the brain. Sci Transl Med 2011; 3:65ps1
10. Irie M, Hata Y, Takeuchi M, Ichtchenko K, Toyoda A, Hirao K, Takai Y, Rosahl TW, Südhof TC: Binding of neuroligins to PSD-95. Science 1997; 277:1511–5
11. Barrow SL, Constable JR, Clark E, El-Sabeawy F, McAllister AK, Washbourne P: Neuroligin1: A cell adhesion molecule that recruits PSD-95 and NMDA receptors by distinct mechanisms during synaptogenesis. Neural Dev 2009; 4:17
12. Chubykin AA, Atasoy D, Etherton MR, Brose N, Kavalali ET, Gibson JR, Südhof TC: Activity-dependent validation of excitatory *versus* inhibitory synapses by neuroligin-1 *versus* neuroligin-2. Neuron 2007; 54:919–31
13. Jung SY, Kim J, Kwon OB, Jung JH, An K, Jeong AY, Lee CJ, Choi YB, Bailey CH, Kandel ER, Kim JH: Input-specific synaptic plasticity in the amygdala is regulated by neuroligin-1 *via* postsynaptic NMDA receptors. Proc Natl Acad Sci U S A 2010; 107:4710–5
14. Peng HY, Chen GD, Tung KC, Lai CY, Hsien MC, Chiu CH, Lu HT, Liao JM, Lee SD, Lin TB: Colon mustard oil instillation induced cross-organ reflex sensitization on the pelvic-urethra reflex activity in rats. Pain 2009; 142:75–88
15. Peng HY, Chen GD, Lai CY, Hsieh MC, Lin TB: Spinal SIRPα1-SHP2 interaction regulates spinal nerve ligation-induced neuropathic pain *via* PSD-95-dependent NR2B activation in rats. Pain 2012; 153:1042–53
16. Peng HY, Hsieh MC, Lai CY, Chen GD, Huang YP, Lin TB: Glucocorticoid mediates water avoidance stress-sensitized colon-bladder cross-talk *via* RSK2/PSD-95/NR2B in rats. Am J Physiol Endocrinol Metab 2012; 303:E1094–106
17. Peng HY, Chen GD, Lai CY, Hsieh MC, Lin TB: Spinal serum- and glucocorticoid-inducible kinase 1 (SGK1) mediates neuropathic pain *via* kalirin and downstream PSD-95-dependent NR2B phosphorylation in rats. J Neurosci 2013; 33:5227–40
18. Tabuchi K, Südhof TC: Structure and evolution of neurexin genes: Insight into the mechanism of alternative splicing. Genomics 2002; 79:849–59
19. Ullrich B, Ushkaryov YA, Südhof TC: Cartography of neurexins: More than 1000 isoforms generated by alternative splicing and expressed in distinct subsets of neurons. Neuron 1995; 14:497–507
20. Hata Y, Butz S, Südhof TC: CASK: A novel dlg/PSD95 homolog with an *N*-terminal calmodulin-dependent protein kinase domain identified by interaction with neurexins. J Neurosci 1996; 16:2488–94
21. Gnanasekaran A, Bele T, Hullugundi S, Simonetti M, Ferrari MD, van den Maagdenberg AM, Nistri A, Fabbretti E: Mutated CaV2.1 channels dysregulate CASK/P2X3 signaling in mouse trigeminal sensory neurons of R192Q Cacna1a knock-in mice. Mol Pain 2013; 9:62
22. Friedman HV, Bresler T, Garner CC, Ziv NE: Assembly of new individual excitatory synapses: Time course and temporal order of synaptic molecule recruitment. Neuron 2000; 27:57–69
23. Nam CI, Chen L: Postsynaptic assembly induced by neurexin-neuroligin interaction and neurotransmitter. Proc Natl Acad Sci U S A 2005; 102:6137–42
24. Prange O, Murphy TH: Modular transport of postsynaptic density-95 clusters and association with stable spine precursors during early development of cortical neurons. J Neurosci 2001; 21:9325–33
25. Graf ER, Zhang X, Jin SX, Linhoff MW, Craig AM: Neurexins induce differentiation of GABA and glutamate postsynaptic specializations *via* neuroligins. Cell 2004; 119:1013–26
26. Heine M, Thoumine O, Mondin M, Tessier B, Giannone G, Choquet D: Activity-independent and subunit-specific

recruitment of functional AMPA receptors at neurexin/neuroligin contacts. Proc Natl Acad Sci U S A 2008; 105:20947–52

27. Zimmermann M: Ethical guidelines for investigations of experimental pain in conscious animals. Pain 1983; 16:109–10
28. Peng HY, Chen GD, Hsieh MC, Lai CY, Huang YP, Lin TB: Spinal SGK1/GRASP-1/Rab4 is involved in complete Freund's adjuvant-induced inflammatory pain *via* regulating dorsal horn GluR1-containing AMPA receptor trafficking in rats. Pain 2012; 153:2380–92
29. Schäfers M, Svensson CI, Sommer C, Sorkin LS: Tumor necrosis factor-α induces mechanical allodynia after spinal nerve ligation by activation of p38 MAPK in primary sensory neurons. J Neurosci 2003; 23:2517–21
30. Hori K, Ozaki N, Suzuki S, Sugiura Y: Upregulations of P2X(3) and ASIC3 involve in hyperalgesia induced by cisplatin administration in rats. Pain 2010; 149:393–405
31. Mayer S, Kumar R, Jaiswal M, Soykan T, Ahmadian MR, Brose N, Betz H, Rhee JS, Papadopoulos T: Collybistin activation by GTP-TC10 enhances postsynaptic gephyrin clustering and hippocampal GABAergic neurotransmission. Proc Natl Acad Sci U S A 2013; 110:20795–800
32. Peng HY, Chen GD, Tung KC, Chien YW, Lai CY, Hsieh MC, Chiu CH, Lai CH, Lee SD, Lin TB: Estrogen-dependent facilitation on spinal reflex potentiation involves the Cdk5/ERK1/2/NR2B cascade in anesthetized rats. Am J Physiol Endocrinol Metab 2009; 297:E416–26
33. Zhao C, Du CP, Peng Y, Xu Z, Sun CC, Liu Y, Hou XY: The upregulation of NR2A-containing *N*-methyl-D-aspartate receptor function by tyrosine phosphorylation of postsynaptic density 95 *via* facilitating Src/proline-rich tyrosine kinase 2 activation. Mol Neurobiol 2015; 51:500–11
34. Mondin M, Labrousse V, Hosy E, Heine M, Tessier B, Levet F, Poujol C, Blanchet C, Choquet D, Thoumine O: Neurexin-neuroligin adhesions capture surface-diffusing AMPA receptors through PSD-95 scaffolds. J Neurosci 2011; 31:13500–15
35. Scheiffele P, Fan J, Choih J, Fetter R, Serafini T: Neuroligin expressed in nonneuronal cells triggers presynaptic development in contacting axons. Cell 2000; 101:657–69
36. Dahlhaus R, Hines RM, Eadie BD, Kannangara TS, Hines DJ, Brown CE, Christie BR, El-Husseini A: Overexpression of the cell adhesion protein neuroligin-1 induces learning deficits and impairs synaptic plasticity by altering the ratio of excitation to inhibition in the hippocampus. Hippocampus 2010; 20:305–22
37. Dolique T, Favereaux A, Roca-Lapirot O, Roques V, Leger C, Landry M, Nagy F: Unexpercted association of the "inhibitory" neuroligin 2 with excitatory PSD95 in neuropathic pain. Pain 2013; 154:2529–46
38. Peng HY, Chang HM, Chang SY, Tung KC, Lee SD, Chou D, Lai CY, Chiu CH, Chen GD, Lin TB: Orexin-A modulates glutamatergic NMDA-dependent spinal reflex potentiation *via* inhibition of NR2B subunit. Am J Physiol Endocrinol Metab 2008; 295:E117–29
39. Peng HY, Chang HM, Lee SD, Huang PC, Chen GD, Lai CH, Lai CY, Chiu CH, Tung KC, Lin TB: TRPV1 mediates the uterine capsaicin-induced NMDA NR2B-dependent cross-organ reflex sensitization in anesthetized rats. Am J Physiol Renal Physiol 2008; 295:F1324–35
40. Chang CH, Peng HY, Wu HC, Lai CY, Hsieh MC, Lin TB: Cyclophosphamide induces NR2B phosphorylation-dependent facilitation on spinal reflex potentiation. Am J Physiol Renal Physiol 2011; 300:F692–9
41. Peng HY, Chen GD, Lai CY, Hsieh MC, Hsu HH, Wu HC, Lin TB: PI3K modulates estrogen-dependent facilitation of colon-to-urethra cross-organ reflex sensitization in ovariectomized female rats. J Neurochem 2010; 113:54–66
42. El-Husseini AE, Schnell E, Chetkovich DM, Nicoll RA, Bredt DS: PSD-95 involvement in maturation of excitatory synapses. Science 2000; 290:1364–8
43. Stein V, House DR, Bredt DS, Nicoll RA: Postsynaptic density-95 mimics and occludes hippocampal long-term potentiation and enhances long-term depression. J Neurosci 2003; 23:5503–6
44. Rowen L, Young J, Birditt B, Kaur A, Madan A, Philipps DL, Qin S, Minx P, Wilson RK, Hood L, Graveley BR: Analysis of the human neurexin genes: Alternative splicing and the generation of protein diversity. Genomics 2002; 79:587–97
45. Rao A, Harms KJ, Craig AM: Neuroligation: Building synapses around the neurexin-neuroligin link. Nat Neurosci 2000; 3:747–9
46. Dean C, Scholl FG, Choih J, DeMaria S, Berger J, Isacoff E, Scheiffele P: Neurexin mediates the assembly of presynaptic terminals. Nat Neurosci 2003; 6:708–16
47. Choi YB, Li HL, Kassabov SR, Jin I, Puthanveettil SV, Karl KA, Lu Y, Kim JH, Bailey CH, Kandel ER: Neurexin-neuroligin transsynaptic interaction mediates learning-related synaptic remodeling and long-term facilitation in aplysia. Neuron 2011; 70:468–81
48. Boucard AA, Chubykin AA, Comoletti D, Taylor P, Südhof TC: A splice code for trans-synaptic cell adhesion mediated by binding of neuroligin 1 to α- and β -neurexins. Neuron 2005; 48:229–36
49. Chih B, Gollan L, Scheiffele P: Alternative splicing controls selective trans-synaptic interactions of the neuroligin-neurexin complex. Neuron 2006; 51:171–8
50. Ichtchenko K, Hata Y, Nguyen T, Ullrich B, Missler M, Moomaw C, Südhof TC: Neuroligin 1: A splice site-specific ligand for β-neurexins. Cell 1995; 81:435–43
51. Futai K, Kim MJ, Hashikawa T, Scheiffele P, Sheng M, Hayashi Y: Retrograde modulation of presynaptic release probability through signaling mediated by PSD-95-neuroligin. Nat Neurosci 2007; 10:186–95
52. Bats C, Groc L, Choquet D: The interaction between Stargazin and PSD-95 regulates AMPA receptor surface trafficking. Neuron 2007; 53:719–34
53. Shi Y, Lu W, Milstein AD, Nicoll RA: The stoichiometry of AMPA receptors and TARPs varies by neuronal cell type. Neuron 2009; 62:633–40
54. Varoqueaux F, Jamain S, Brose N: Neuroligin 2 is exclusively localized to inhibitory synapses. Eur J Cell Biol 2004; 83:449–56
55. Levinson JN, Chéry N, Huang K, Wong TP, Gerrow K, Kang R, Prange O, Wang YT, El-Husseini A: Neuroligins mediate excitatory and inhibitory synapse formation: Involvement of PSD-95 and neurexin-1β in neuroligin-induced synaptic specificity. J Biol Chem 2005; 280:17312–9